KU Leuven, Hydraulic laboratory
Kasteelpark Arenberg 40, PB 2448
B-3001 Heverlee

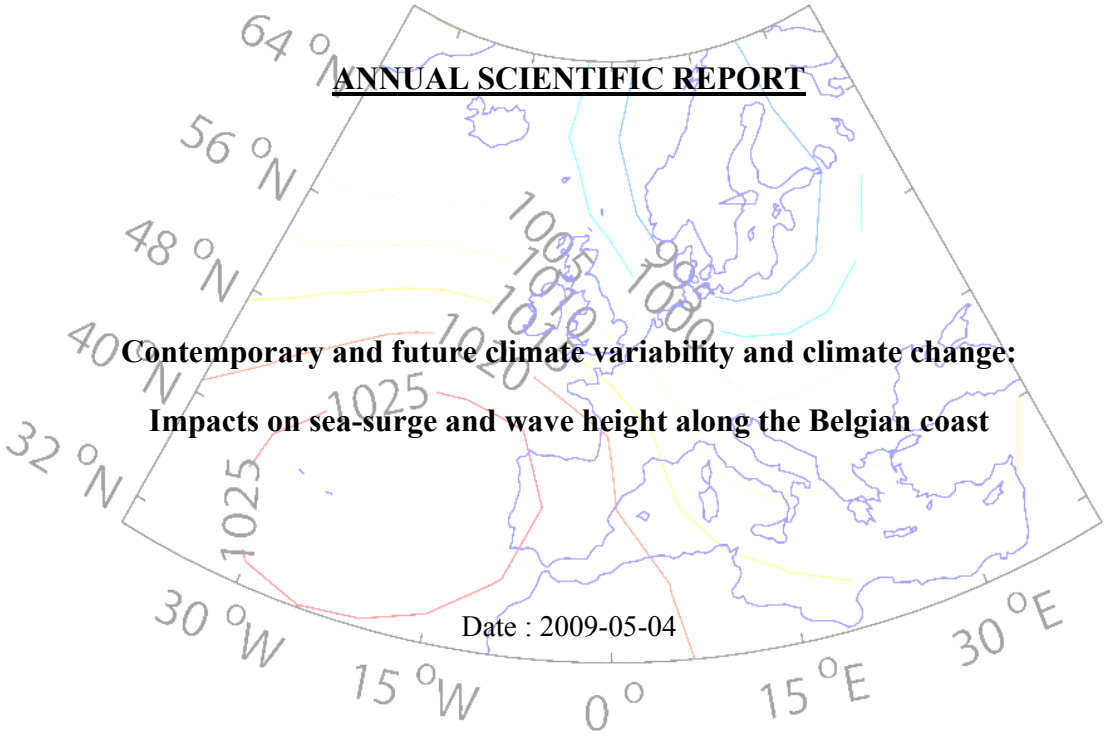

ANNUAL SCIENTIFIC REPORT

Contemporary and future climate variability and climate change:

Impacts on sea-surge and wave height along the Belgian coast

Date : 2009-05-04

AUTHOR(S):

- Albin Ullmann, KU Leuven
- Jaak Monbaliu, KU Leuven

OTHER PARTNERS:

- Dries Van den Eynde, Management Unit of the North Sea Mathematical Models
- Andreas Sterl, KNMI, the Netherlands

Table of Contents

Table of Figures

Table of Tables

1 Introduction

1.1 General and literature overview

Coastal management is increasingly concerned by the future climate variability and its impact on extreme sea levels and waves. Recent climatic models summarized by the Intergovernmental Panel on Climate Change (IPCC) have predicted a significant warming and global sea-level rise for the 21st century (IPCC, 2007), which is expected to increase the flooding risk along low lying coasts. Various factors may induce sea level variations at different time scales. On time scales longer than 1 year, regional and global scale sea level variations are related to volume change due to seawater density change, associated with temperature and salinity variations (Tsimplis and Rixen, 2002; Cazenaves and Nerem, 2004) and mass change between Ocean and continents, including ice melting (Lambeck, 1990; Cabanes *et al*., 2001). On time scales of less than 1 year, the predominant forcing of sea level variations is mostly related to atmospheric variability (Pirazzoli, 2000; Svensson and Jones, 2002; Wakelin *et al*, 2003; Ullmann *et al*., 2008). The atmospheric forcing leads to (i) high waves and (ii) sea surges defined as the difference between the observed sea level and the astronomical tide at the same moment. To summarize, **extreme water levels observed at one moment correspond to the superimposition of a surge or a wave height on a mean sea level**.

A rise of the mean sea-level during the next century seems to be inevitable, mostly because of the temporal inertia and the time of response of Seas and Oceans to the global warming observed during the last decades. IPCC designed different stories for our future climate based on SRES-scenarios for the 21st century. Within these climate change scenarios, the mean sea-level could rise between + 1 mm/yr and + 9 mm/yr (IPCC, 2007). Although the future mean sea-level rise will be mainly linked with the increase of the sea surface temperature, several other parameters could play a role, especially at regional scale: oceanic circulation, salinity, continental ice melting which are still difficult to predict. The main uncertainties about future extreme sea levels come from storminess because clear relations between local key processes and large scale climate variability are difficult to obtain. Further problems occur because a changing climate may cause changes in the relationship between global and local parameters use to predict storminess at regional scale. The assessment of local impacts is therefore very difficult. In fact, a review of the existing literature shows that studies gives sometimes contradictory conclusions.

A way of dealing with the uncertainties is to summarize the literature and synthesize the actual knowledge on the change of hydraulic and physical parameters in the southern North Sea coming from neighbouring countries (Netherlands, United Kingdom and Germany). This work has been done by the CLIMAR partners (Management Unit of the North Sea Mathematical Models, Arcadis Ecolas, Maritime Institute of Ghent University, Flanders Hydraulics Research, Instituut voor Landbouw en Visserij Onderzoek). Three long-term scenarios for

2100 are presented in table 1. The three scenarios include a moderate scenario (M), a warm scenario (W) and a more improbable 'worst-case' scenario (Worst). The first two scenarios (M, W) are first divided further in a scenario where no significant differences in the air circulation could be expected, confirming results of some previous studies for the North Sea (Van den Hurk *et al.*, 2006; Sterl *et al.*, 2008). Following results show by other studies (Low *et al.*, 2001; Debenard *et al.*, 2002), these scenarios are then divided further in scenario where the air circulation could change significantly (M+, W+). Note that the sea level rise in the last improbable 'worst case' scenario, accounts for some unexpected but possible effects, such as the massive melting of ice sheets and the stopping of the thermohaline Ocean Circulation. This last scenario was proposed by Brooks *et al.* (2006).

	M	M+	W	W+	Worst
Air temperature	+ 2° C	+ 2° C	+ 4° C	+ 4° C	+ 4° C
Change air circulation	No	Yes	No	Yes	Yes
Wind velocity	0 %	+ 4 %	- 2 %	+ 8 %	+ 8 %
Sea water temperature	+ 2,5 °C	+ 2,5 °C	+ 3,5 °C	+ 3,5 °C	+ 3,5 °C
Mean sea level	+60 cm	+ 60 cm	+93 cm	+93 cm	+200 cm

Table 1. Scenarios of climate change for the 21st century and sea-level and atmospheric parameters related variability.

1.2 Objectives

Storm-related surges and waves along the Belgian coast are complex local events linked with winds and atmospheric pressure. The purpose of our study is thus to develop a regional-scale strategy focuses for the Belgian coast to (i) better understand the relationship between storm surges and the atmospheric circulation and (ii) to robustly predict the long-term variability of extreme surge height in future climate. A downscaling approach is used to build a statistical relationship between surge height, which are required by impact researchers but not adequately described in Global and Regional Circulation Models, and large-scale features well resolved (von Storch, 1999). After an overview of the data used for this study (section 2) the relationship between sea-level pressure (SLP) and surges and wave height along the Belgian coast is first analyzed during the 20th century (section 3). Following these relationship, linear statistical models are used to relate the interannual variability of surge height with SLP (section 4). Statistical models are then used to forecast changes in surge and wave height along the Belgian coast under different climate change scenarios (section 5). In conclusion, we propose two potential climate change scenarios for storminess and sea-level rise for the Belgian coast for the 21st century.

2 Data: description and validation

2.1 Sea-level pressure

2.1.1 ERA-40 & NCAR reanalysis in the 20th century

➢ European Center for Medium Weather Forecast (ECMWF) Reanalysis (ERA-40) mean sea level pressure (SLP) at 0, 6, 12 and 18h UTC have been extracted from the ECMWF web site (http://www.ecmwf.int/) from 1958 to 2000 and over [40°W-40°E]-[30°N-70°N]. Data are available on a 2.5° * 2.5° regular latitude-longitude grid.

➢ Mean sea level pressure available from National Center for Atmospheric Research (NCAR) at 1 p.m. UTC from October 1, 1925 to December 31, 1939 and at noon UTC from January 1, 1940 to March 31, 2000 has been extracted from the NCAR web site (http://dss.ucar.edu/) over [40°W-40°E]-[30°N-70°N]. Data are available on a 5° * 5° regular latitude-longitude grid.

ERA-40 dataset has been enhanced by the ECMWF and NCAR dataset by the National Center for Atmospheric Research. These two datasets are built with many sources of observations provided by different countries and organizations. An optimal spatial interpolation has been done for area where data are not available (Kalnay *et al*., 1996). No attempt has been made to fill the missing entries in data or to remove the seasonal cycle.

2.1.2 GCM numerical simulations

➢ Two 6-hourly SLP time series simulated by ARPEGE-climat (coupled global circulation model) were provided by Meteo France (Royer *et al*., 2002). The first run simulates data from 1980 to 2100 and was driven by the scenario A2 of 21st Greenhouse Gases (GHG) concentration from the IPCC Special Report on Emission Scenario (SRES). This scenario assumes a rapid increase of atmospheric concentration of GHG until the end of the 21st century. The second run gives data from 1950 to 2100 and was driven by the scenario B2 which is a more optimistic than A2. In fact, this scenario predict a rapid increase of the atmospheric concentration of GHG until 1950 but foresees then a small decline until the end of the 21st century, assuming a rapid development of sustainable and renewable energy. During the historical period, runs are forced by observed concentrations of GHG and anthropogenic aerosols. For the future, aerosols and solar irradiance are kept constant while GHG keep rising according to SRES scenario A2 (respectively B2) until 2100. Gridded-SLP data are extracted over [40°W-40°E]-[30°N-70°N] and have been extrapolated on the same regular spatial resolution than NCAR.

- A basic ensemble of 17 runs of 6-hourly SLP time series simulated from 1950 to 2100 were provided by A. Sterl from the Royal Netherland Meteorological Institute (KNMI). The ECHAM/MPI-OM (Jungclaus *et al*., 2006) coupled global circulation model of the Max-Planck Institute for Meteorology was used because it performed well on a number of criteria during an intercomparison of models that were considered in the IPCC fourth Assessment Report (AR4). In fact, in preparation of this AR4 report, a number of modeling centers have performed runs with their coupled climate models. A comparison in terms of atmospheric circulation revealed the coupled ECHAM/MPI-OM as one of the better of these models in terms of the global and regional circulation patterns (Van Ulden and Van Oldenborgh, 2006). All runs were driven by the SRES scenario A1b (between scenario A2 and B2) which is currently considered as the most likely climate change scenario for the 21st century. The storyline describes a future world with of very rapid economic growth, global population that peaks in mid-century and declines thereafter, and the rapid introduction of new and more efficient technologies (IPCC, 2007). During the historical period (1950-2000), runs are forced by observed concentrations of GHG and anthropogenic aerosols. For the future, GHG keep rising according to SRES scenario A1b until 2100. For the 17-ensembles runs, the model has been driven by the same scenario but with 17 different model initializations to make more robust estimates of the model's forced response compare to the natural chaotic climate variability. This experiment has been done in the ESSENCE project (Sterl *et al*., 2008) where a large-member ensemble of runs with a state-of-the-art climate model is performed to investigate the range of possible future climate change. Gridded-SLP data are extracted over [40°W-40°E]-[30°N-70°N] and have been extrapolated on the same regular spatial resolution than NCAR.

2.1.3 GCMs: control experiment

For each grid-point over [40°W-40°E]-[30°N-70°N], the mean SLP difference has been computed for the period 1950-2000 between NCAR dataset and (i) each 17-ensembles runs of ECHAM/MPI-OM and (ii) for ARPEGE single run B2. A Student t-test is performed for each grid-point to check if the statistical significance of the difference. No significant differences of the mean SLP condition were found over the Baltic Sea and the Azores (figure 1). For both GCM, significant differences in the mean SLP condition are only northward from 56°N (figure 1) around Iceland that confirms that the ECHAM/MPI-OM climate model performs well in most of the terms of global and regional circulation patterns (Marlsand *et al*., 2003; Van Oldenborgh *et al*., 2005; Van Ulden and Van Oldenborgh, 2006).

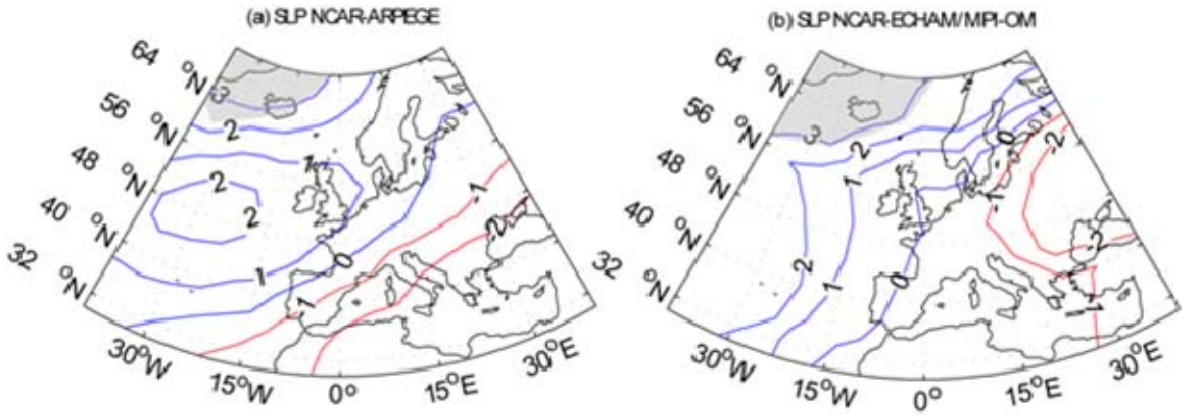

Figure 1. Mean SLP difference (in hPa) computed between yearly mean SLP of NCAR dataset minus (a) the yearly mean SLP averaged for the 17-ensembles runs simulated with ECHAM/MPI-OM GCM and (b) the yearly mean SLP simulated with ARPEGE GCM (scenario B2 only) for the period 1950-2000. Shading indicates significant values at the 99% level of confidence according to a student's t-test.

Mean stormtracks have been computed for the period 1950-2100 for NCAR dataset, for the mean of the 17-ensembles runs and for the single ARPEGE run B2. Stormtracks are computed as the standard deviation of the daily SLP field over [40°W-40°E], [30°N-70°N]. Daily SLP has been first high-pass filtered (Butterworth, 1930) to retain only periods between 2 and 6 days which correspond to the usual lifetime of extra-tropical storms (Orlanski, 1975). In this way, an important standard deviation indicates a large variability of SLP and this variability is mostly associated with the activity of extratropical storms. First of all, the maximum standard deviation in NCAR dataset only differs from +1 hPa compared to the two GCMs (figure 2). It means that ARPEGE and ECHAM/MPI-OM perform well the SLP deviation. Then, the location of the maximum standard deviation is almost similar between NCAR and the two GCMs and always between [48°N-56°N] and [40°W-30°W] (figure 2).

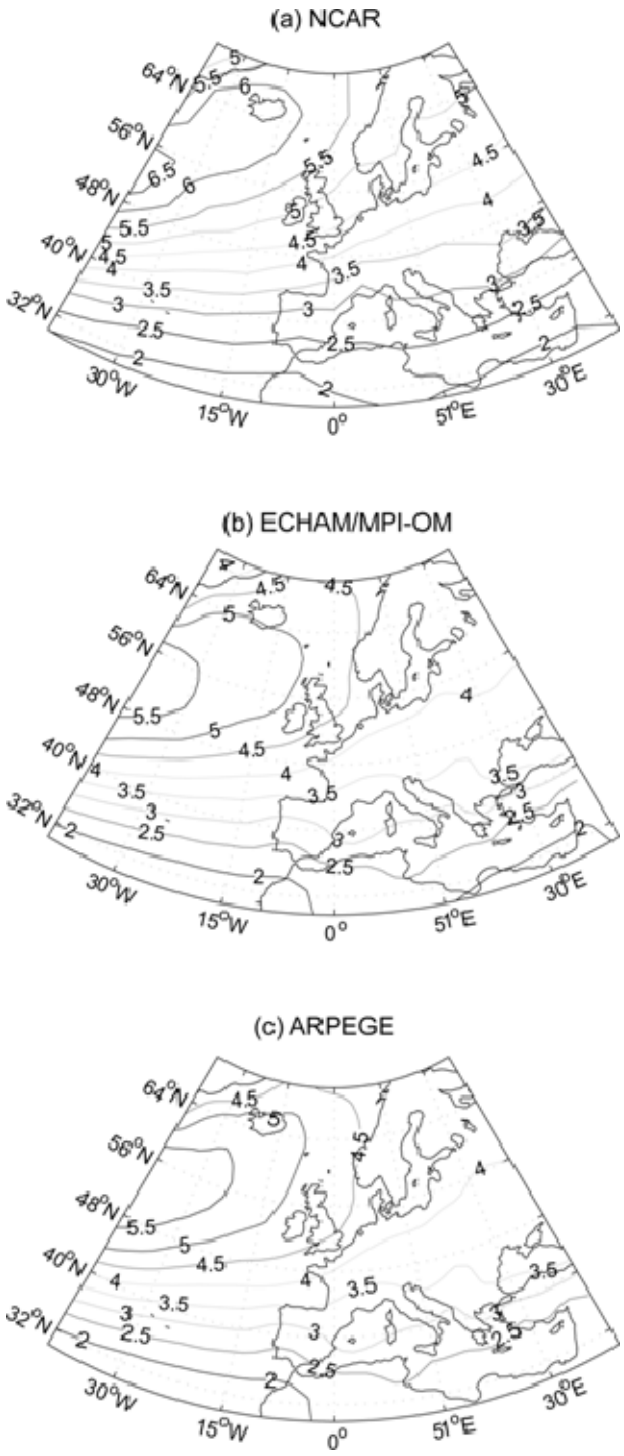

Figure 2. Stormtracks: standard deviation of high-pass daily SLP retaining only periods between 2 and 6 days for (a) NCAR dataset, (b) mean the 17-ensembles runs and (c) for ARPEGE A2 run for the period 1950-2000.

2.2 Sea level, sea-surge and waves height

2.2.1 Daily maximum sea-level height at Oostende ([02°54'E], [51°13'N])

Time series along Belgian coast from 1925 to 2000. Data are expressed in cm relatively to the same altimetry reference level TW (*Twerde Algemene Waterpassing)*. For each daily maximum sea level, the corresponding astronomical tide (in TAW) has been computed in a previous study by Technum-IMDC-Alkyon (2002). The daily sea-surge height has been computed as **the difference between the observed sea level and the astronomical tide at the same moment**. As daily surges are derived from the daily maximum sea level, they always correspond to surges occurring during high tide which is particularly interesting in an impact perspective. Moreover, the study of the interannual to multi-decadal variability of surge-height lead to the decision to separate the problem of the mean sea level (MSL) trend and the problem of the isolated spiked (the surges) (Pirazzoli *et al*., 2005). In other words, sea-level variability associated with atmospheric circulation (i.e. sea surges) needs to be separated from sea-level variability associated with volume changes due to temperature and salinity variations and mass change between ocean and continent. Therefore, for each year, the value of the yearly mean of daily maximum sea-level is removed from daily surge heights. The different climatic aspects estimated this way are kept independent as much as possible **and interannual variability to long-term trend of surge can be separated from ocean volume variations** (Pirazzoli *et al*., 2005).

2.2.2 Significant wave height

Significant wave heights (Hm0) measured by buoy at Oostende (1997-2001), Westhinder (1994-2001) and Akkaert (1997-2001) were collected and will be used for the analysis in section 3. Data values are available every 15 min.

2.2.3 WAQUA: surge-height numerical simulation

A basic ensemble of 17 runs of 10-minutes surge height time series simulated from 1950 to 2100 were provided by the Royal Netherland meteorological institute (KNMI). Runs were computed with the WAQUA-in-Simona / DCSM98 storm surge model, developed by the National Institute for Coastal and Marine Management, Delft University and KNMI. The model calculates the surge height using wind and pressure forecasts. The 17 WAQUA's runs were driven by an ensemble of 17 runs of wind speed and atmospheric pressure simulated by the ECHAM/MPI-OM coupled global circulation model under SRES scenario A1b (see section 2.1.2). A test run has been made by the KNMI using ERA-40 wind and atmospheric pressure interpolated to the same ECHAM/MPI-OM grid. The resulting surge heights

compare well with observations meaning that the cross-resolution forcing (i.e. downscaling between GCM's forcing and local surge height) provide enough information to simulated realistic local-scale surges. During the historical period (1950-2000), runs are driven by wind and atmospheric pressure simulated by ECHAM/MPI-OM forced by observed concentrations of GHG and anthropogenic aerosols. For the future, aerosols and solar irradiance are kept constant while GHG keep rising according to SRES scenario A1b until 2100. Data are analyzed at 6 locations in the North Sea, from France to the Netherlands: Dunkirk, Zeebrugge, Oostende, Vlissingen, Westkapel, and Hoekvanholland. First of all, runs have been performed without tidal forcing to keep only the surge component. Then, they have been then preformed including tidal forcing to simulate 17 runs of 10-minutes total sea-level height.

2.2.4 WAQUA: control experiment

Statistical distribution of surge height recorded at Oostende tide-gauge station and for the 17-ensembles WAQUA's runs have been analyzed for the period 1950-2000 (only one daily value is considered). The Kurtosis coefficients (measure of whether the data are peaked or flat) are quite similar between observations and the WAQUA's simulations at Oostende (table 2). The skewness (measure of the symmetry) is slightly higher in WAQUA than in the observations. It means that positive surges simulated with WAQUA are over-represented compared to the observations (table 2). The mean standard deviation of the 17 runs (= 26.7 cm) is almost **equal to the standard deviation of observations at Oostende** (=24.7 cm). Moreover, amplitude between the maximum and the minimum surge is almost similar between observations and simulations (table 2). Nevertheless, surges in WAQUA are usually higher than the observations. The mean surge at Oostende for the period 1950-2000 is equal to - 3.58 cm and the average of the 17 WAQUA's runs is equal to + 3.8 cm (table 10), meaning that surges in WAQUA meanly upper-estimated surges at Oostende of +7.38 cm. **To maximize to consistency between observation and simulation, we withdraw 7.38 cm to all values of the 17 surge-height time series at Oostende simulated with WAQUA.**

	Max. (cm)	Min. (cm)	Amp. (cm)	Std. (cm)	Mean (cm)	Kurt.	Skew.
Oostende observations	219	-167	386	24.7	-3.58	5.8	0.47
Waqua (mean of the 17 runs)	221	-174	395	26.7	3.8	5.2	0.63

Table 2. Statistics of the surge height at Oostende for the period 1950-2000 derived from *in situ* observations and from the WAQUA's 17-ensembles runs. Max.: maximum surge, Min.: minimum surge, Amp.: amplitude between maximum and minimum, Std.: standard deviation, Mean: the mean surge, Kurt.: the Kurtosis coefficient and Skew.: the skewness coefficient

	Data	Area and spatial resolution	Source	Time scale
ERA-40	Sea-level pressure (hPa)	[40°W-40°E]-[30°N-70°N] 2.5°*2.5°	Reanalyzes	. 6-hourly . 1950-2000
NCAR	Sea-level pressure (hPa)	[40°W-40°E]-[30°N-70°N] 2.5°*2.5°	Reanalyzes	. Daily . 1925-2000
ESSEMBLE	Sea-level pressure (hPa)	[40°W-40°E]-[30°N-70°N] 2.5°*2.5°	Simulations: ECHAM/MPI-OM, 17- ensembles runs, A1b scenario	. 6-houlry . 1950-2100
ARPEGE	Sea-level pressure (hPa)	[40°W-40°E]-[30°N-70°N] 2.5°*2.5°	Simulations: ARPEGE, 1 run A2 & 1 run B2 scenario	. 6-hourly . 1950-2100 (B2) . 1980-2100 (A2)
Oostende	. Sea level (TAW) . Sea surge (cm)	Oostende	Tide gauge measurements	. Daily . 1925-2000
Hm0	Significant wave height (TAW)	. Oostende . Westhinder . Akkaert	Buoy measurements	. 15-min . 1997-2001 . 1994-2001 . 1997-2001
WAQUA	. Sea level (TAW) . Sea surge (cm)	. Dunkirk . Zeebrugges . Oostende .Vlissingen . Westkapel . Hoekvanholland	Simulations: WAQUA, A1b scenario	. 10-min . 1950-2100

Table 3. Overview of the data available

3 Sea surges and waves height along the Belgian coast during the 20th century

3.1 Spatial variability

15-minutes wave-height time series have been correlated between each pair of station from 1997 to 2000. Moreover, the daily maximum wave height at each buoy station has been correlated with the daily surge height at Oostende for the period 1997-2000. Student's t-test was used to test if the linear correlation is significantly different from zero. First of all, the wave-height variability shows a linear relationship between Oostende, Westhinder and Akkaert even at the 15-minute time scale (table 4). **Second also the correlation between daily maximum wave height and daily surge height show a significant relationship (table 4).**

	Oostende	Westhinder	Akkaert	Surge at Oostende
Oostende	1	-	-	-
Westhinder	0.96***	1	-	-
Akkaert	0.92***	0.98***	1	-
Surge at Oostende	0.62***	0.55***	0.60***	1

Table 4. Correlation between 15-minutes wave-heights at Oostende, Westhinder and Akkaert for the period 1997-2000. Last line: correlation between the daily maximum wave height and the daily surge height at Oostende for the period 1997-2000. Three stars indicate that the correlation is significant et the 99% level of confidence according to a Student's t-test.

Daily maximum wave heights were averaged at each station for different daily sea-surge ranges at Oostende and for the period 1997-2000. It is clear that wave height increase with positive surge height (figure 3). It's interesting to note that wave height also increase with strong negative surges (figure 3). In fact, strong positive and negative surge are both associated with strong winds pushing the water either toward or far from the coast but in the mean time, these strong wind also create large waves. To summarize, it means that **wave and surge height vary at regional-scale and are associated with atmospheric conditions acting at a larger spatial scale than the Belgian coast**.

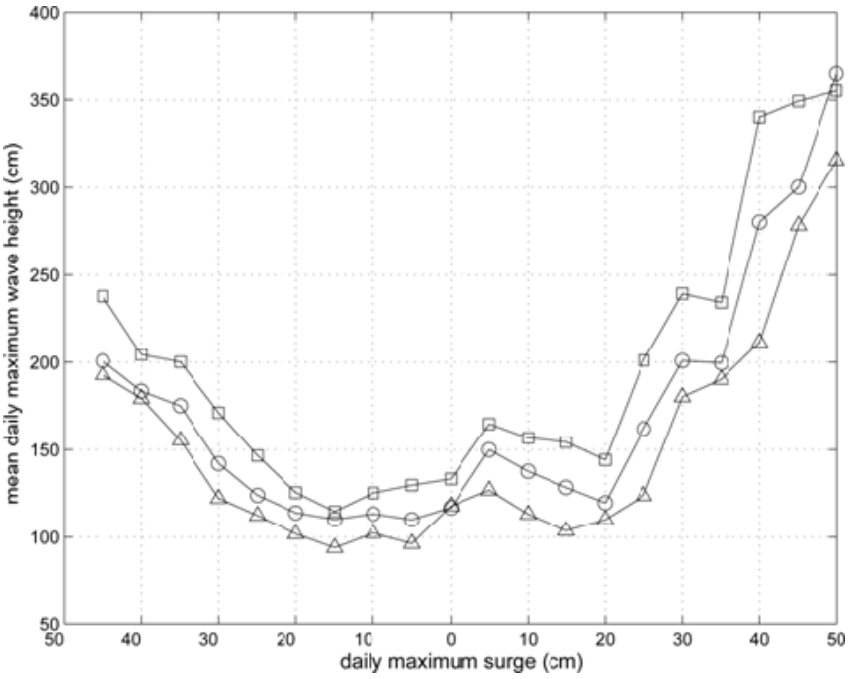

Figure 3. Daily maximum wave height averaged at Oostende (line with circle), Akkaert (line with square) and Westhinder (line with triangle) for daily sea surge at Oostende different height for the period 1997-2000.

3.2 Atmospheric conditions of extreme events

For each grid-point over [40°W-40°E]-[30°N-70°N], correlation has been computed (i) between the daily surge height at Oostende and the daily SLP for the period 1950-2000 and (ii) between 6-hourly SLP and the corresponding wave height at Westhinder for the period 1994-2000. Figure 4 shows **a clear relationship between surge and wave height along the Belgian coast and the SLP over the Baltic Sea ([15°-20°E], [50°-55°N])**. Note that the correlation between the daily surge height and the daily SLP over the Belgian coast is rather weak ($-0.2 < r < -0.3$; figure 4), meaning that surge height variability at Oostende not directly linked with SLP variability over the Belgian coast. In other words, even if the inverted barometric effect (i.e. 1 cm surge-height variability for 1 hPa just-above SLP change) plays a role in the surge-height variability at daily time scale (Pirazzoli *et al*., 2005), it is not the main atmospheric forcing for Belgian surges.

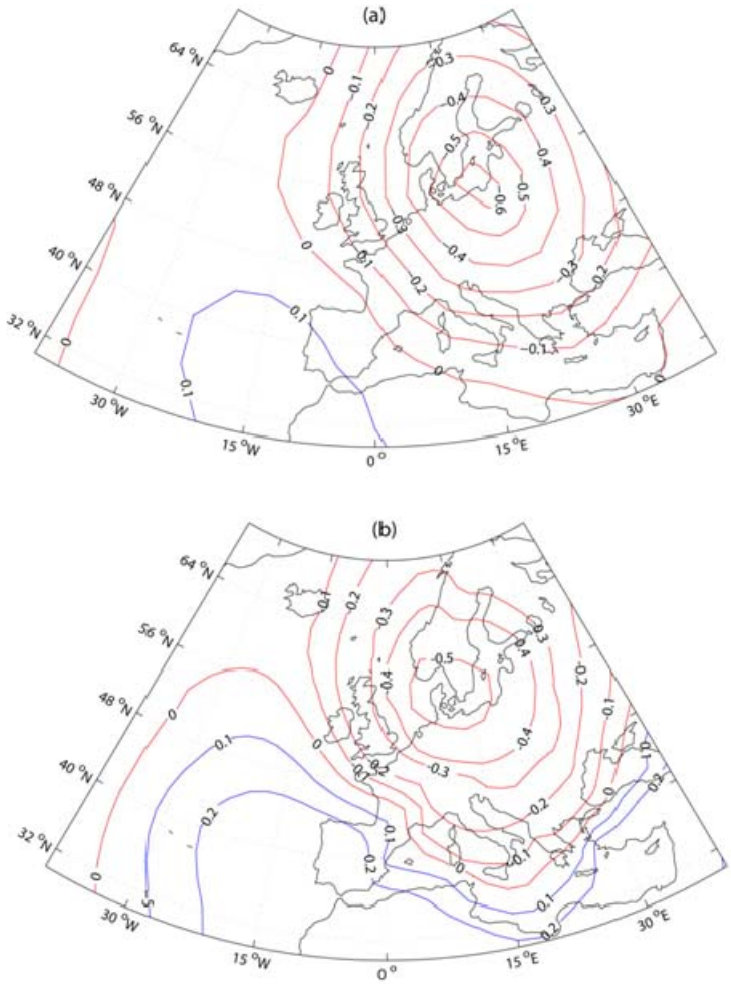

Figure 4. (a) Correlation between daily surge height at Oostende and the NCAR SLP for the period 1950-2000. (b) Correlation between 6-hourly ERA-40 SLP and the corresponding wave height at Westhinder for the period 1994-2000.

A composite analysis was performed to determine the regional-scale atmospheric circulation associated with the highest surges and waves following Trigo and Davies (2002). The composites of the mean SLP for each day when daily surges are above 35 cm (i.e. the 90th percentile of daily surge height for the period 1950-2000) were computed for the following time lags: 5, 4, 3, 2, 1 and 0 days (figures 5 and 5). The same composites were computed when daily maximum wave heights at Westhinder are above 2.5 m (i.e. the 90th percentile of daily maximum wave height for the period 1994-2000). When a surge (wave) event encompasses several days, the day with the highest surge (wave) was considered as day 0. This composite analysis does not make any specific assumptions regarding the link between SLP and surge and wave height, but simply estimates the mean SLP pattern conditional on the highest surges and waves.

Atmospheric circulation associated with highest surges and waves along the Belgian coast are almost similar (figure 5 and 6). During the 6-day window shown in figure 5 and 6, the main synoptic storm track in the North Atlantic–European sector follows a west to east axis, from the southern tip of Greenland (figure 5a, 6a) toward Scandinavia (figure 5f, 6f). During the same period, the low-pressure system intensifies, particularly from day(−2) to day(−1) (figure 5c-e, 6c-e), as it moves to the east. Associated with a reinforced Azores high, the Northeast-Southwest gradient across the North-Sea is rather strong from day(−1), and the low-pressure system typically reaches its minimum SLP over the northern tip of the Baltic Sea 1 day before the highest surge at Oostende. This SLP pattern favors strong onshore winds, from Northwest sectors in the southern North Sea, and the piling up of water along Belgian coast. These results are fully consistent with the relationship between extreme sea surges and waves along the southern coasts of the North-Sea and the “Scandinavia type” shown by Petersen and Rohde in 1991.

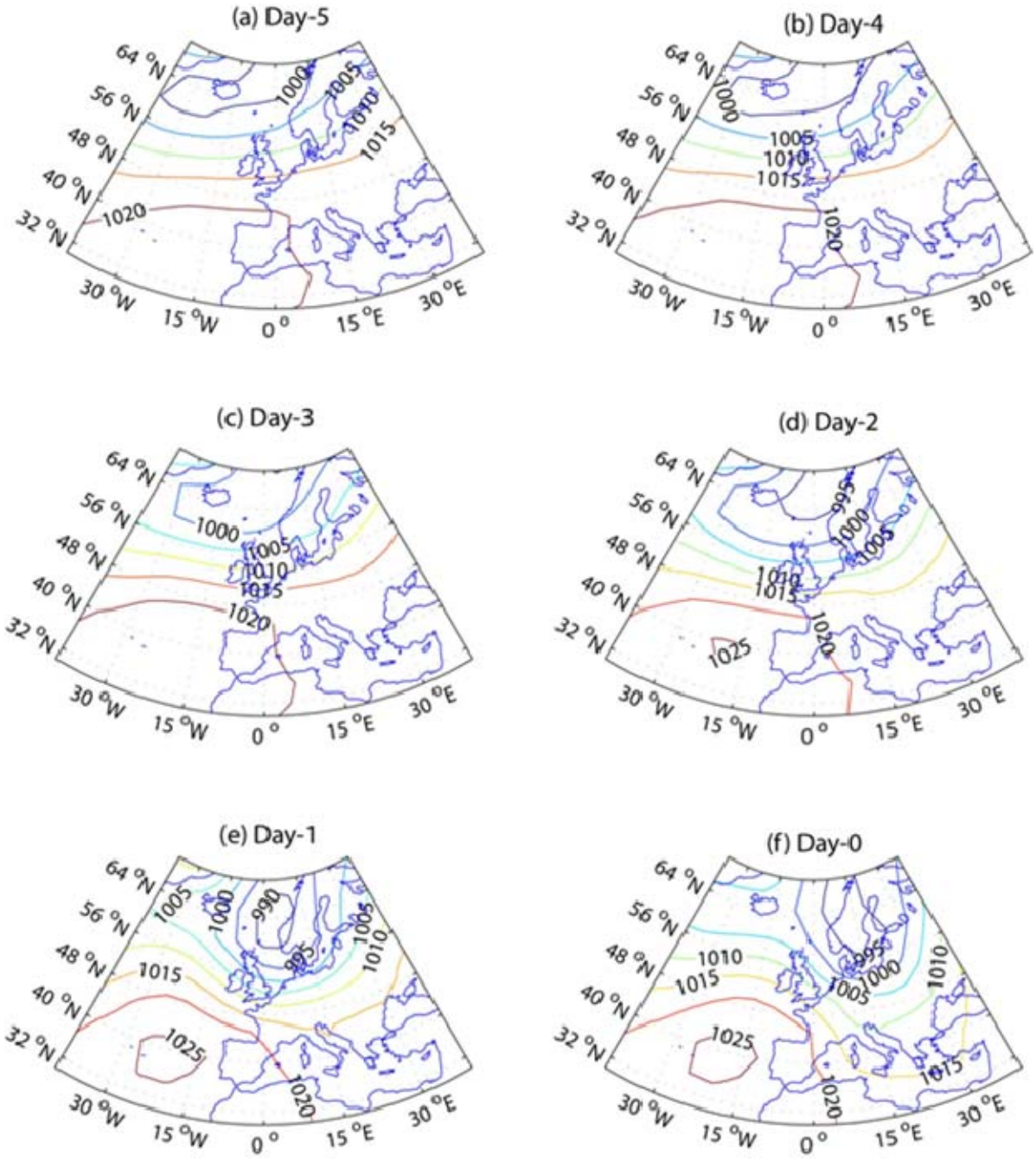

Figure 5. Mean NCAR SLP for daily surges at Oostende > 35 cm and at time lag of (a) 5 days, (b) 4 days, (c) 3 days, (d) 2 days, (e) 1 days for the period 1950 to 2000.

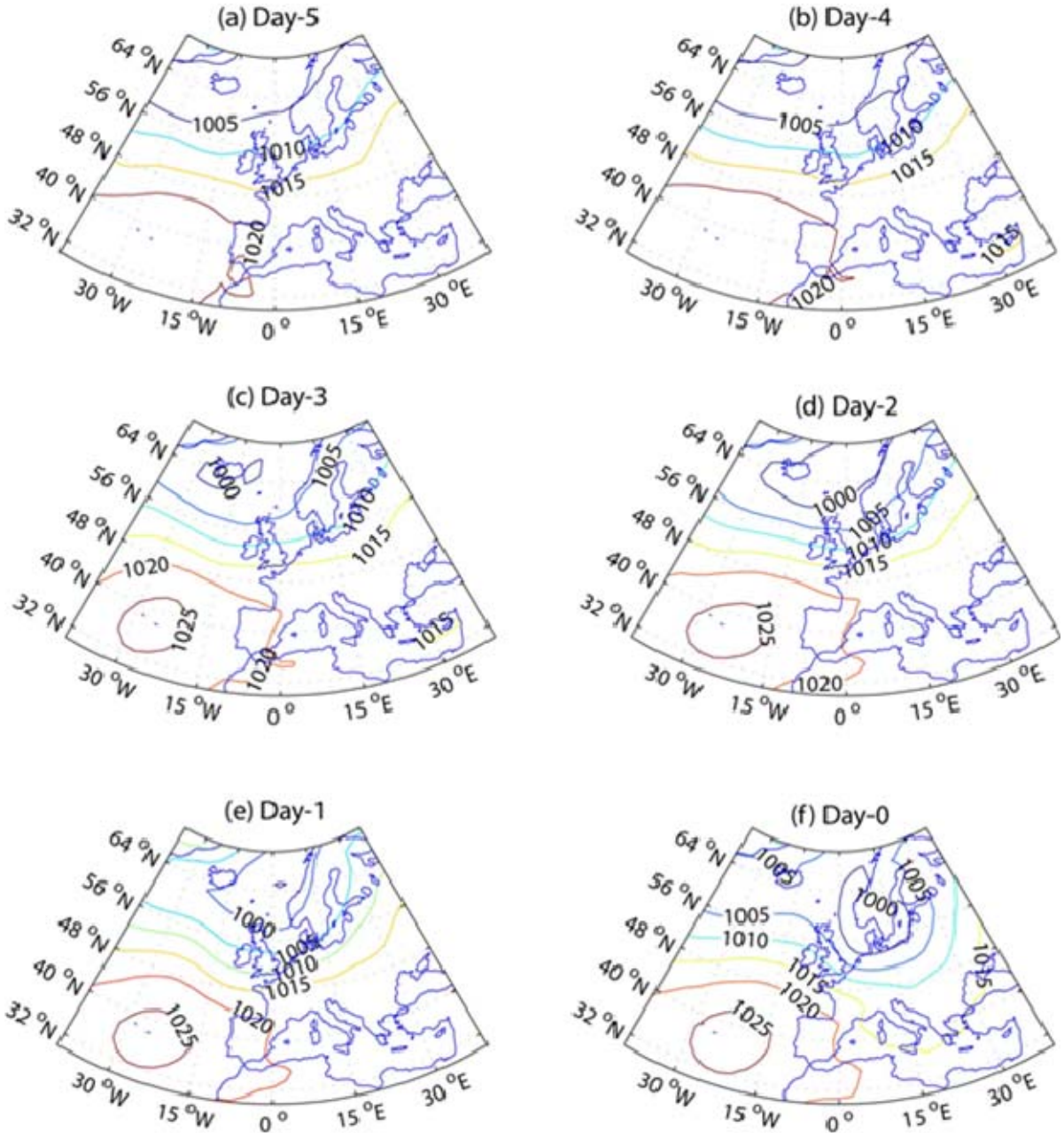

Figure 6. Mean NCAR SLP for daily maximum wave height at Westhinder > 2.5 m and at time lag of (a) 5 days, (b) 4 days, (c) 3 days, (d) 2 days, (e) 1 days for the period 1994 to 2000.

3.3 Interannual to multi-decadal variability in the 20th century

The yearly 99th percentiles of daily maximum sea level and the corresponding daily sea surge have been computed at Oostende from 1925 to 2000. Yearly 99th percentile of maximum sea level shows an increasing trend of + 3.2 mm/yr, significant over 99% level of confidence with a Student's T test (figure (7a). During the same period, the yearly 99th percentile of daily sea surge has increased at a rate of + 1.3 mm/yr (p > 99%) but especially from ~1955-60 to 1980 (figure 7b). Surge height tends then to slightly decrease until the beginning of the 21st century. Over the whole available period, the yearly mean of the daily maximum sea level shows a continuous rise at a rate of + 2.0 mm/yr (figure 7c) consistent with the mean trend observed (~ 2 mm/yr) in the whole southern North Sea during the 20th century (Siegismund and Schrum, 2001; Weisse *et al*., 2005). To summarize, long-term increase in yearly 99th percentile of sea-level height at Oostende (i.e. extreme sea levels) during the 20th century could be explained as the superimposition of (**i) the increase of yearly 99th percentile of sea surges**, partly associated with increase of onshore NW winds and storminess in the southern North Sea, especially between 1960 and 1980 (Alexandersson *et al*., 2000; Weisse *et al*., 2005) on **(ii) the slow mean sea-level rise**, mostly linked with the increase in sea surface temperature and the related thermal expansion (Nerem and Mitchum, 2001; Cazenave and Nerem 2004, CLIMAR, 2007).

In the CLIMAR project of the Belgian Science Policy (evaluation of climate change impacts and adaptation responses for maritime activities) the longest available wave-height time series have been analyzed for the Belgian and the Dutch coast. A clear statistically significant long-term trend is not visible for the period 1980-2007. Nevertheless, for most stations along the Belgian coast, a small decrease is found in extreme wave height (CLIMAR, 2007). This variability of wave height is consistent with **(i) the decrease in surge height observed at Oostende from ~1980 (figure 5b) and (ii) the slight decrease in wind speed in the southern North Sea during the last two decades** (CLIMAR, 2007; Van den Eynde *et al*., 2008). To summarize, daily to multi-decadal surge and wave height variability are strongly correlated to each other.

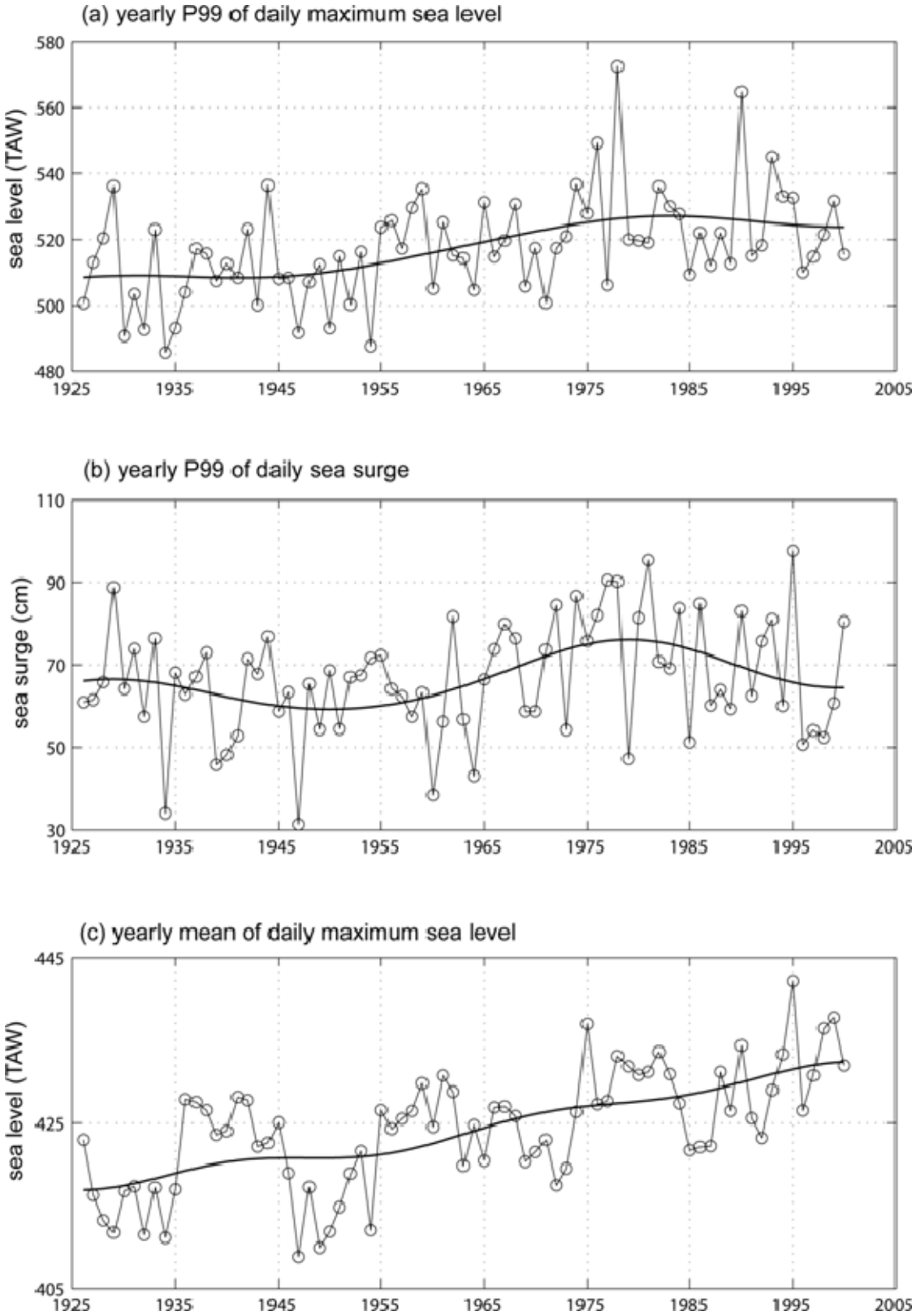

Figure 7. (a) Yearly 99th percentile of daily maximum sea level at Oostende from 1925 to 2000. (b) Yearly 99th percentile of daily sea surge and (c) yearly mean of the daily maximum sea level with the low-pass variations (period > 30 years) superimposed as full line.

We observed that the highest sea surges and waves are associated with a strong southwest-northeast pressure gradient between high pressure around the Azores [30°-0°W], [35°-45°N] and low pressure over the Baltic Sea ([15°-20°E], [50°-55°N]). Figure 8 displays the low-pass filtered variability (only periods longer than 1/30 cycle-per-year) of the yearly mean SLP averaged over these two area. Figure 8b shows a clear increase of the SLP over the Atlantic, between 35°N and 45°N, particularly from ~1960 to 1980, consistent with the increase of the Azores high and the positive deviation of the North-Atlantic Oscillation shown in previous studies (Hurell and Van Loon, 1997; Machel *et al*., 1998). The behaviour of the SLP over the Baltic Sea is less monotonous and shows clear multi-decadal oscillations (figure 8a). Nevertheless, over the whole available period the linear trend doesn't show a significant linear evolution (figure 8a). The yearly frequency of strong daily barometric gradient between low pressure < 990 hPa over the Baltic Sea and high pressure < 1020 hPa over the Azores increases during the 20th century and particularly between 1960 and 1980 (figure 8c), synchronous with the SLP rise over the Azores (figure 8b). This increase is **consistent with the increase in sea-surge height and wind speed during the same period** (figure 7; Alexandersson *et al*., 2000; Weisse *et al*., 2005). Then, the yearly frequency of such daily barometric gradient slightly decreases until the beginning of the 21st century (figure 8c) consistent with the weak decrease of surge height, wave height and wind speed in the southern part of the North Sea during the last two decades of the 20th century (CLIMAR, 2007).

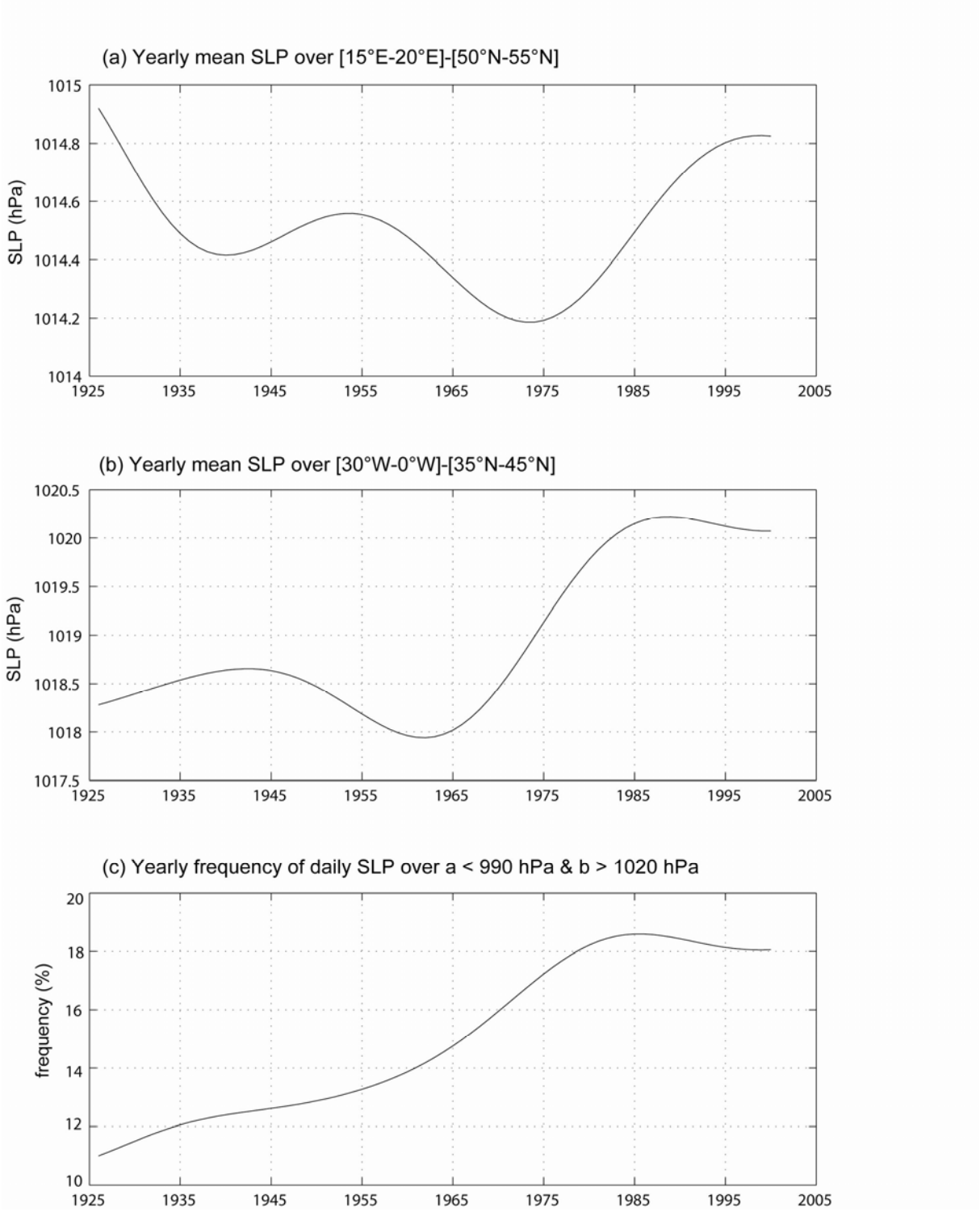

Figure 8. (a) low-pass filtered (period > 30 years) yearly mean sea-level pressure (SLP) averaged over the Baltic Sea [15°E-20°E], [50°N-55°N] and over the Azores (b) [30°W-0°W], [35°N-45°N] for the period 1925-2000 period. Low-pass filtered yearly frequency of days with SLP > 1020 hPa over [30°E-0°E], [35°N-45°N] and SLP < 990 hPa over [15°-20°E], [50°-55°N].

3.4 Climate change and surge-height variability during the 20th century

Increase in surge height between 1960 and 1980 could be partly associated with the SLP rise over the Azores. This large-scale and long-term barometric variability leads to the question of climate change and natural variability. Climate change (contrary to natural variability) is defined as the part of climate variability associated with external forcing such as aerosols and greenhouse gases. In this study, we try to present answer the difficult question of the "attribution" of the SLP rise over the Azores and thus to analyze if the increase in surge height along the Belgian coast during the second half of the 20th century could be associated with climate change.

ARPEGE and ECHAM/MPI-OM are two ocean-atmosphere coupled GCMs which simulate their own ocean and own Sea Surface Temperature (SST). Like all GCMs, they are chaotic (as well as the climate system). It means that they cannot reproduce the real chronology of the climate variability except the chronology associated with external forcing as aerosol and Greenhouse gases. One important point here is that ECHAM/MPI-OM model has been driven by the same scenario A1b but with 17 different model initializations to make more robust estimates of the model's forced response compare to the natural chaotic climate variability. Remember that on the historical period (i.e. 1950-2000), all runs are forced by observed concentrations of GHG and anthropogenic aerosols. Therefore, we assume that if the SLP rise over the Azores in the second half of the 20th century is associated with climate change (i.e. increase in atmospheric concentration of GHGs), GCMs should simulate this increase.

Yearly mean SLP averaged over the Baltic Sea ([15°E-20°E], [50°N-55°N]) and over the Azores ([30°W-0°W], [35°N-45°N]) have been computed with (i) NCAR dataset, (ii) the 17-ensembles runs A1b and (ii) the single run B2 for the period 1950-2000. Figure 9 shows the slow variability of yearly mean SLP over the Azores according to a Butterworth filter retaining only period above 30 years (Butterworth, 1930). In the second half of the 20th century, the yearly mean SLP over the Azores simulated by both GCMs and each scenario show a small increase and especially until ~1980 consistent with the observed SLP rise (figure 9a-b). Nevertheless, the amplitude of the SLP rise observed over the Azores reaches 2 hPa between 1960 and 1980 while the increase simulated by GCMs is only between +0.4 hPa and +0.6 hPa (figure 9b). Note that 12 of the 17-ensembles runs shows a SLP rise over the Azores until ~1980, 3 runs show stationary SLP and 2 runs show a weak decrease of the mean SLP over the Azores during the period 1950-2000. Following these results, we could make the assumption that the SLP rise over the Azores observed between 1960 and 1980 could be mostly linked with the natural variability of the climate system and partly with the increase in the atmospheric concentration of aerosols and GHGs. This hypothesis is consistent with previous studies showing that the SLP rise over the Azores could be partly associated with increase in oceanic SST (Rodwell *et al*., 1999). To summarize, the most important part of the increase in surge height along the Belgian coast in the second half of the 20th century, associated with the SLP rise over the Azores, is obviously mostly associated with natural variability of the climate system and only partly with climate change.

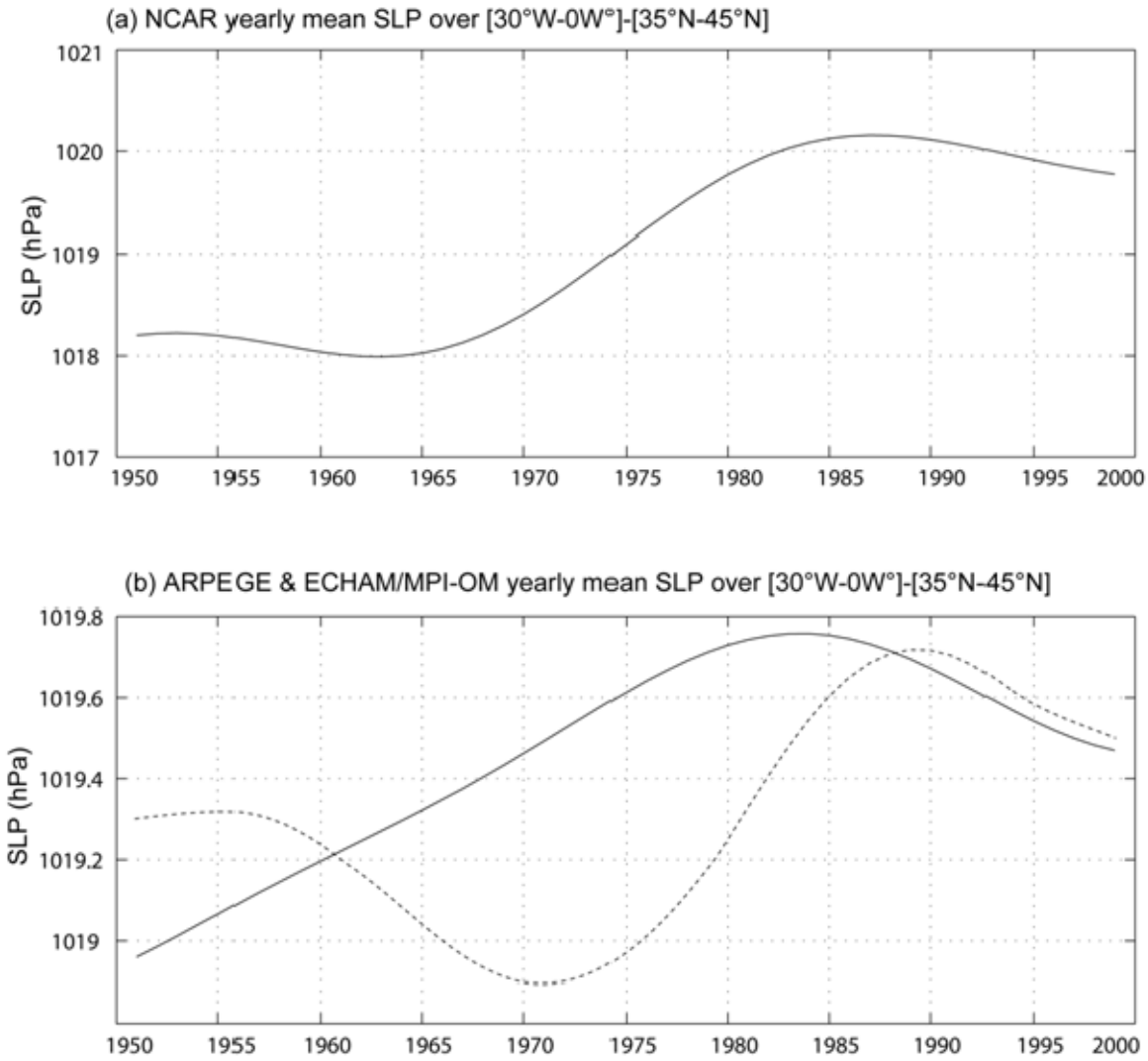

Figure 9. Low-pass filtered (period > 30 years) yearly mean SLP averaged over [30°W-0°W], [35°N-45°N] for the period 1950-2000 for (a) NCAR dataset and (b) for the 17-ensembles runs (full line) and for the single run B2 (dashed line).

Figure 10 shows the slow variability of yearly mean SLP over the Baltic Sea. In the second half of the 20th century, temporal slow variability of simulations is not synchronous with observations (figure 10a-b). For example, the SLP rise of more than 1 hPa between 1975 and 2000 is not simulated by GCMs, neither in ARPEGE nor in ECHAM/MPI-OM (figure 10a-b). In fact, only one of the 17-ensembles runs shows a SLP rise over the Baltic Sea during the period 1950-2000. In seems thus that the slow variability of the SLP over the Baltic Sea for the period 1950-2000 is almost only associated with the natural variability of the climate system.

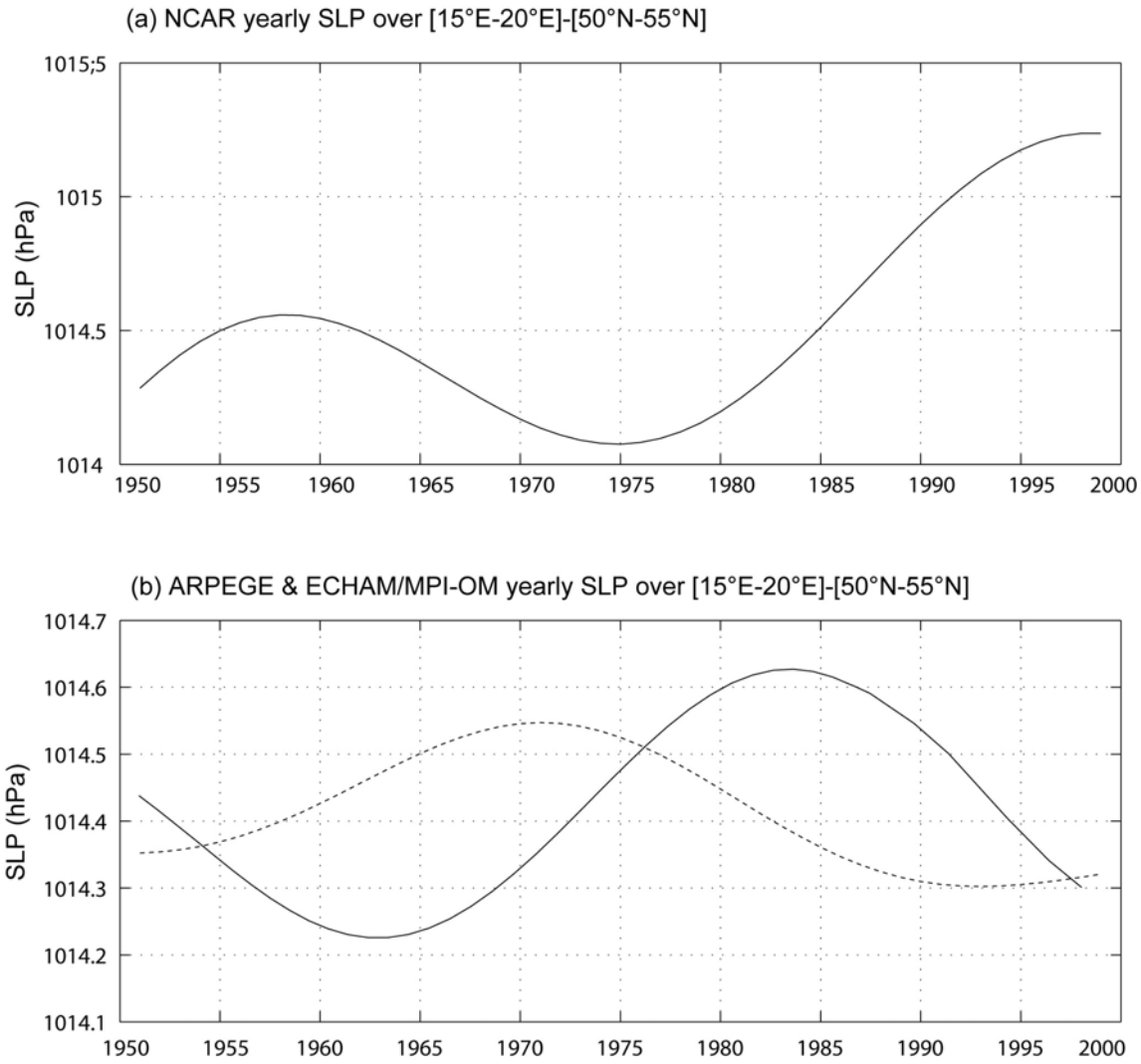

Figure 10. Low-pass filtered (period > 30 years) yearly mean SLP averaged over [15°W-20°W], [50°N-55°N] for the period 1950-2000 for (a) NCAR dataset and (b) for the 17-ensembles runs (full line) and for the single run B2 (dashed line).

4 Sea surges, wave heights and climate conditions: models and prediction for the 21st century

Coupled atmosphere-ocean general circulation models are used to produce numerical simulations of several variables and for different SRES scenarios. However, they are designed to resolve phenomena of several hundred kilometers, and not always reliable below this scale. Consequently, regional coastal systems are not resolved sufficiently in these models. Downscaling techniques, based on statistical relationships between global and regional parameters are therefore required to analyze the impact of climate change at regional-scale. A regional-scale downscaling strategy has been developed here to simulate and predict the height, frequency and duration of sea-surges along the Belgian coast in a future climate.

4.1 Statistical downscaling in the 20th century

4.1.1 Model set-up

There has been considerable interest and concern regarding the interannual and long-term variation of the amplitude of sea surges and their dependence on SLP variability. Many studies, focusing on the German Bight have demonstrated the strong link between the intramonthly percentiles of sea surges and the seasonal SLP over the eastern North Atlantic (i.e. Heyen *et al*., 1996; von Storch and Reichardt, 1997; Langenberg *et al*., 1999). Following results presented in section 3.2, two SLP indexes are designed as predictors of surge height along the Belgian coast:

- The first one is the daily SLP averaged over the Baltic Sea ([15°E-20°E], [50°N-55°N]) which is quasi-linearly correlated with the daily surge height at Oostende (figure 4, section 3.2);
- The second one is the daily value of the pressure gradient between the SLP averaged over the Baltic Sea ([15°E-20°E], [50°N-55°N]) and over the Azores ([30°W-0°W], [35°N-45°N]), corresponding to the difference between the highest and the lowest SLP area observed during extreme sea surges at Oostende (section 3.2). Moreover, this pressure gradient is clearly linked with the direction and strength of the strongest surge-related atmospheric flow. This gradient has been empirically fitted in order to find the best correlation with the daily surge height at Oostende.

Simple linear regressions are first designed for the period 1950-2000 to relate daily surge height at Oostende to *(1)* daily SLP averaged over the Baltic Sea and *(2)* daily value of the pressure gradient between the SLP averaged over the Baltic Sea and the Azores. A multiple linear regression *(3)* is then tested in order to relate daily surge height at Oostende to both of these two atmospheric predictors.

$$DS_1 = (a_1 * BS) + cst_1 \qquad (1)$$

$$DS_2 = (a_2 * GRA) + cst_2 \qquad (2)$$

$$DS_3 = (a_3 * BS) + (b_1 * GRA) + cst_3 \qquad (3)$$

With coefficients *a*, *b* and *cst* (i.e. constant value), coefficients of the regression and with *DS*, hindcast daily surge height (in cm), *BS* the daily sea-level pressure (in hPa) average over the Baltic Sea and *GRA*, the daily value of the pressure gradient (in hPa) between SLP averaged over the Baltic Sea and the Azores for the period 1950-2000. In many applications, the predictor does not completely specify the predictand (von Storch, 1999). In a prediction perspective, hindcast time series need to have the same standard deviation as the observations. To meet this requirement, it has been proposed to inflate the hindcast by setting a coefficient

of inflation (Karl *et al*., 1990). For each hindcast daily surge-height time series, a coefficient of inflation has been computed as the ratio between the standard deviation of observed and hindcast daily surge height. This technique has been used in the downscaling literature to some extent (e.g. Huth, 1999). After inflation, observed and hindcast daily surge heights have the same standard deviation. All the coefficients are summarized in table 5.

For each hindcast daily surge-height time series, the monthly 90th (P90), 95th (P95) and 99th (P99) percentile of surge is computed and compared with *in situ* observation at Oostende. Note that percentile values are computed from a polynomial curve fit (6th order) to the empirical cumulative distribution function (cdf). We choose here the monthly 90th (95th and 99th) percentile of surge height, defined as the value for which 90 (95 and 99) percent of all daily surges are less than it, as an indicator of monthly highest (extreme) surges. We employ standard descriptive measures of goodness-of-fit, including the root-mean-square error (RMSE) to evaluate the accuracy of the simulated percentiles. RMSE represents overall error weighted by the square of deviations (von Storch and Zwiers, 1998). We also consider the linear correlation *r* between observed and simulated percentiles. Mean and standard deviation (Std) of simulated and observed percentiles are also calculated. In a perfect simulation, in which simulations matches exactly the observations, r=1 and RMSE=0. For inconsistent simulation, r ~ 0 and the RMSE can be up to twice the observed Std (von Storch and Zwiers, 1998). Linear trends of the monthly P90 are also computed for the period 1950-2000 to test the performance of the three statistical models in long-term trends simulations.

Regression *(1)*			
a_1	cst_1	IF_1	
-1.2	1182.2	1.66	
Regression *(2)*			
a_2	cst_2	IF_2	
-0.92	-7.47	1.76	
Regression *(3)*			
a_3	b_1	cst_3	IF_3
-0.89	-0.26	899.4	1.65

Table 5. Coefficients of the regressions (*a*, *b* and *cst*) and coefficient of inflation (*IF*). Regression *(1)*: for the linear regression using daily SLP averaged over the Baltic Sea as the predictor of daily surge height during the period. Regression *(2)*: for the linear regression using daily value of the pressure gradient between the Baltic Sea and the Azores as the predictor of daily surge height during the period. Regression *(3)*: for the multiple linear regression using both predictor *(1)* and *(2)* during the period 1950-2000.

4.1.2 Results

For the period 1950-2000, the mean of daily surges is almost similar between hindcast and observations (table 6). At a daily time scale, correlation between hindcast and observed daily surge height are almost similar. Nevertheless, coefficients are higher when using (i) only the daily SLP averaged over the Baltic Sea and (ii) both the daily SLP averaged over the Baltic Sea and the daily value of the pressure gradient between SLP over the Baltic Sea and the Azores as predictor of daily surge height (figure 11; table 6). Moreover, it's interesting to note that the multiple linear regression doesn't perform better than the simple linear regression using SLP over the Baltic Sea (table 2). Daily surge-height variability along the Belgian coast is thus mostly linked with the SLP variability over the Baltic Sea (table 2), consistent with results shown in section 3.2. In fact, daily SLP variability over this area (overall over Scandinavia) potentially modified the strength and direction of the atmospheric circulation over Northern Europe and thus wind conditions along the Belgian coast (section 3.2). Moreover, SLP variability over the Baltic Sea generates SLP changes over the Belgian coast and the associated inverted barometric effect which is also important at daily time scale.

	Oostende obs.	Regression *(1)*	Regression *(2)*	Regression *(3)*
Mean of daily surge	-2.8 cm	-3.4 cm	-3.1 cm	-3.4 cm
r obs. vs hindcast		0.61***	0.56***	0.61***

Table 6. First line: the mean daily surge height at Oostende computed for the period 1950-2000 with *in situ* observation and with the daily surge height simulated with the regression *(1)* using the daily SLP averaged over the Baltic Sea, *(2)* the daily value of the pressure gradient between the SLP averaged over the Baltic Sea and the Azores and *(3)* both of these two atmospheric indexes as predictors and after inflation. Second line: correlation between daily observed surge height at Oostende and daily surge height computed with linear regression with *(1)*, *(2)* and *(3)* and after inflation during the period 1950-2000. Three stars indicate that the correlation is significant at the 99% level of confidence with a Student's t-test.

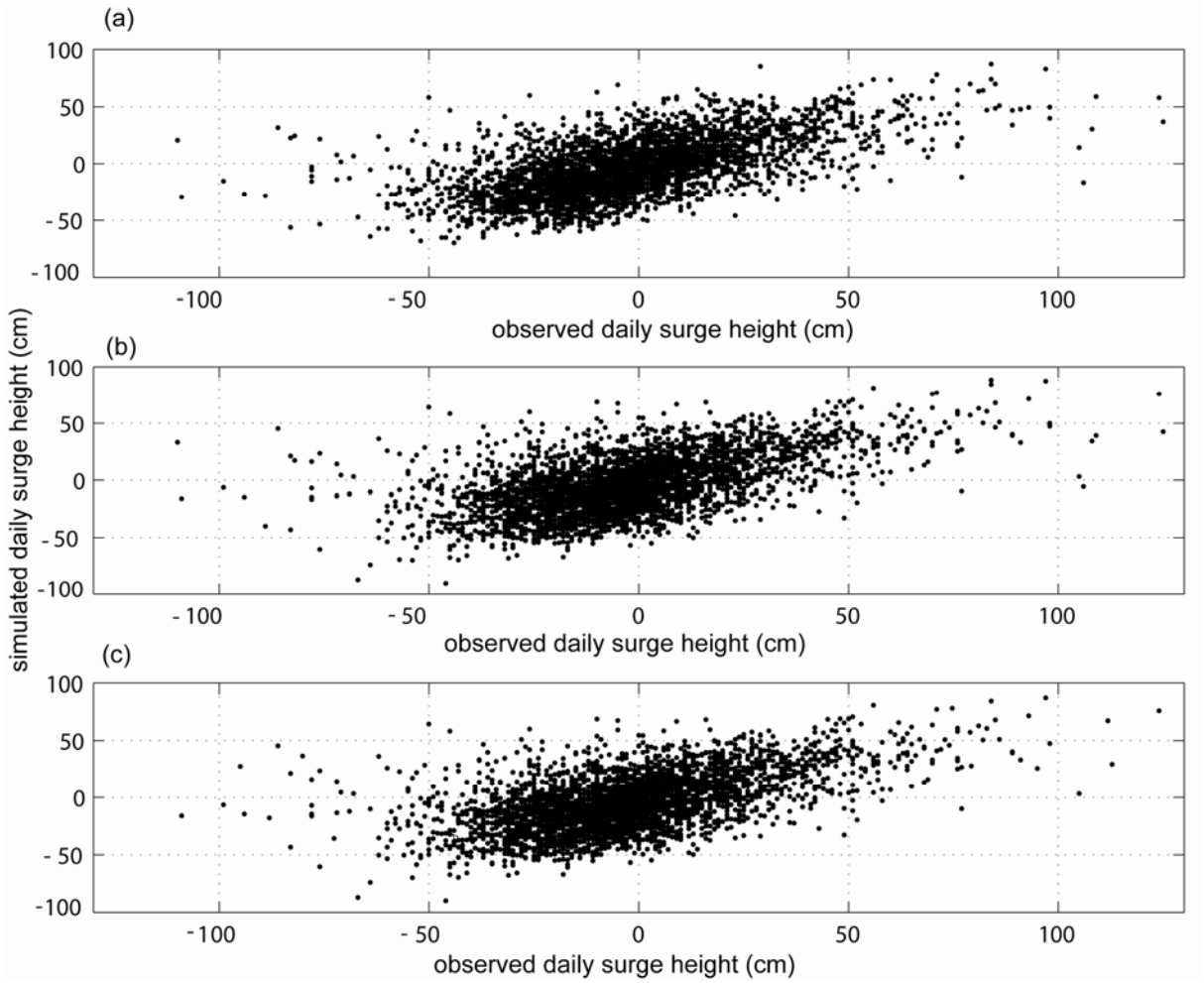

Figure 11. Scatter plot between daily surge height observed at Oostende and daily inflated surge height simulated with the linear regression with (a) the daily SLP averaged over the Baltic Sea (regression 1), (b) the daily value of the pressure gradient between the SLP averaged over the Baltic Sea and the the Azores (regression 2) and (3) both of these two atmospheric index as the predictor (regression 3).

Monthly P90, P95 and P99 of surge are extracted for each daily surge-height time series computed with the three linear regressions and results are compared with observations at Oostende. The agreements between observed and hindcast monthly P90 is very strong for each linear regression (table 7). In fact, correlation coefficients are always > 0.73 significant over 99% level of confidence (table 7). Moreover, moderate RMSE indicates weak uncertainties about the individual hindcast (table 7). For highest surges, inverted barometric effect is not the main forcing of the surge amplitude but mostly the strength of the northeastward barometric gradient between low pressure over the Baltic Sea and high pressure over the Azores, which is directly linked with the direction and speed of northwesterly onshore winds over the Belgian coast (section 3.2). Nevertheless, statistical skills (correlation and RMSE) are always weakly lower when considering linear regression *(2)* using only the pressure gradient between the Baltic Sea and the Azores as the predictor. Once again, statistical skills are almost similar between regressions *(1)* and *(3)* even if this last regression simulates 3% more of common variance with observation than the linear regression

using only SLP over the Baltic Sea as the only predictor. Using both predictors (i.e. the SLP over the Baltic Sea and the barometric gradient between SLP over the Baltic Sea and over the Azores) in the same linear regression doesn't significantly improve the simulation of the interannual variability of the monthly P90 of surges at Oostende compared to the simple linear regression using only SLP over the Baltic Sea as the predictor. The same results are valid when considering the monthly P95 and p99 (table 7). It means that from daily to interannual time-scale, the relationship between highest surge height and the barometric gradient is quasi exclusively linked with the SLP variability over the Baltic Sea and not with the SLP over the Azores. Note that performances of each regression decrease for the simulation of monthly P95 and P99 (table 7). The agreements between observed and hindcast monthly P95 is still robust with significant correlation and moderate RMSE (table 7). Nevertheless, when considering the monthly P99, correlation between hindcast and observation significantly decrease and the RMSE reaches more than 20 cm (table 7). To summarize, linear statistical model, based on downscaling approach, performs well the simulation of the interannual variability of highest surges, but usually underestimates the most extreme values. It's a recurring and normal skew of the linear statistical models.

	r (observation vs simulation)	**RMSE (cm)**	**Mean (cm)**		**Std. (cm)**	
			Obs	**Sim**	**Obs**	**Sim**
Monthly P90						
regression (1)	0.75***	9.1	23.19	23.6	13	13.1
regression (2)	0.73***	11	23.19	21.3	13	16.1
regression (3)	0.77***	9.1	23.19	23.4	13	14.5
Monthly P95						
regression (1)	0.65***	14.1	34.5	30.4	17.3	15.1
regression (2)	0.63***	14.3	34.5	28.3	17.3	16.7
regression (3)	0.66***	13.7	34.5	30.6	17.3	15.5
Monthly P99						
regression (1)	0.49**	22.6	51.5	39.2	25.5	17.3
regression (2)	0.51**	22.7	51.5	38.3	25.5	18.8
regression (3)	0.57**	20.1	51.5	42.1	25.5	18.7

Table 7. Goodness-of-fit statistics of the monthly 90th (P90), 95th (P95), and 99th (P99) percentile estimated with linear regressions and after inflation for the period 1950-2000. Regression *(1)*: with daily SLP averaged over the Baltic Sea as predictors of daily surge heights. Regression *(2)*: with daily value of the pressure gradient between the SLP averaged over the Baltic Sea and over the Azores as predictors of daily surge height. Regression *(3)*: with both of these two atmospheric indexes as the predictors. Two (three) stars indicate that the correlation is significant over 95% (99%) level of confidence with a Student's t-test.

Linear trends are then computed from 1950 to 2000 for the monthly P90 simulated by the linear regressions *(1)* and *(3)*. Results are compared with the linear trend computed with in situ observation at Oostende station, which equals to + 1.2 mm/year. When considering linear regression *(1)* using only SLP averaged over the Baltic Sea as predictor, monthly P90 shows an insignificant increase of + 0.04 mm/year. The multiple linear regression *(3)*, using both SLP averaged over the Baltic Sea and the value of the pressure gradient between the Baltic Sea and the Azores, shows a significant increase of the monthly P90 of + 1.1 mm/years, which is almost similar to the observed trend. The same results were found when considering the P95 and P99 (not shown).

Climatically speaking, strong onshore winds leading to highest surge along the Belgian coast are mainly generated by a strong Northeast-Southwest gradient between low pressure over the Baltic Sea and high pressure over the Azores. Daily to interannual variability of this pressure gradient is quasi exclusively associated with SLP variability over the Baltic Sea and not with over the Azores. In fact, from daily to interannual time scales, SLP over the Azores is particularly stable associated with a large subtropical semi-permanent centre of high pressure, while SLP over the Baltic is strongly variable because it is under the main storm tracks (Rogers, 1997). Nevertheless, over the long-term, changes in the value of the pressure gradient between the Baltic Sea and the Azores could modify the frequency and strength of the surge-related atmospheric circulation over the North Sea. In fact, increase of SLP over the Azores from 1960 to 1980 has increase the yearly frequency of strong northeast-southwest pressure gradient between the Baltic Sea and the Azores and increase the amplitude of highest surge at Oostende station (Ullmann and Monbaliu, 2009). To summarize, highest surges along the Belgian coast are mainly generated by stationary deep low pressure systems over the Baltic Sea and the associated northwesterly winds (i.e. winds turning anticlockwise around the low pressure system in the northern hemisphere). Over the long-term, SLP variability over the Azores also plays a role in the multi-decadal to secular surge-height variability. The multiple linear regression using both daily SLP over the Baltic Sea and the daily value of the pressure gradient between the Azores and the Baltic Sea as predictors of daily surge height at Oostende shows thus the best performance in term of simulation of surge-height variability, from daily time-scale to long-term trend.

4.1.3 Cross-validation

Following conclusions of the previous section, the multiple linear regression (with the daily SLP averaged over the Baltic Sea and the daily value of the pressure gradient between the Azores and the Baltic Sea as predictors of daily surge height at Oostende) is kept for all coming analyzes. The regression is cross-validated to avoid artificial skill due to 'overfitting' (Michaelsen, 1987; von Storch and Zwiers, 1999). Cross-validation is one approach to estimate how well the model we learned from training data is going to perform on future as-yet-unseen data. This is accomplished by dividing the SLP and the surge data into validation

and learning subsets. The coefficient of the regression and the coefficient of inflation have been first learned for the period 1950-1974 and tested for the period 1975-2000. Learning and validation periods have been then reversed and all coefficients are summarized in table 8.

	a	*b*	*cst*	*IF*
1950-1974	-0.96	-0.22	968.3	1.65
1975-2000	-0.83	-0.31	842.5	1.66

Table 8. Coefficients of the regressions (*a*, *b* and *cst*) and coefficient of inflation (*IF*). Second line: when the coefficient of the regression are learned for the period 1950-1974.Third line: when the coefficient of the regression are learned for the period 1975-2000.

At daily time scale, correlation between hindcast and *in situ* surge height at Oostende (1975-2000) is significant (r = 0.61) over 99% level of confidence according to a Student t-test. Monthly 90th percentiles have been then extracted from the inflated daily surge-height time series computed by the regression and compared with *in situ* observations at Oostende (figure 12 and table 9). The agreement between observed and hindcast monthly 90th percentile is very strong (figure 12 and table 9). In fact, the intraseasonal and intreannual variability is correctly reproduced by our statistical model (figure 12a). Moderate RMSE indicates weak uncertainties about the individual hindcasts (table 9). The same robust statistical skills were found when we reversed the learning and the validation periods (figure 12b and table 9):

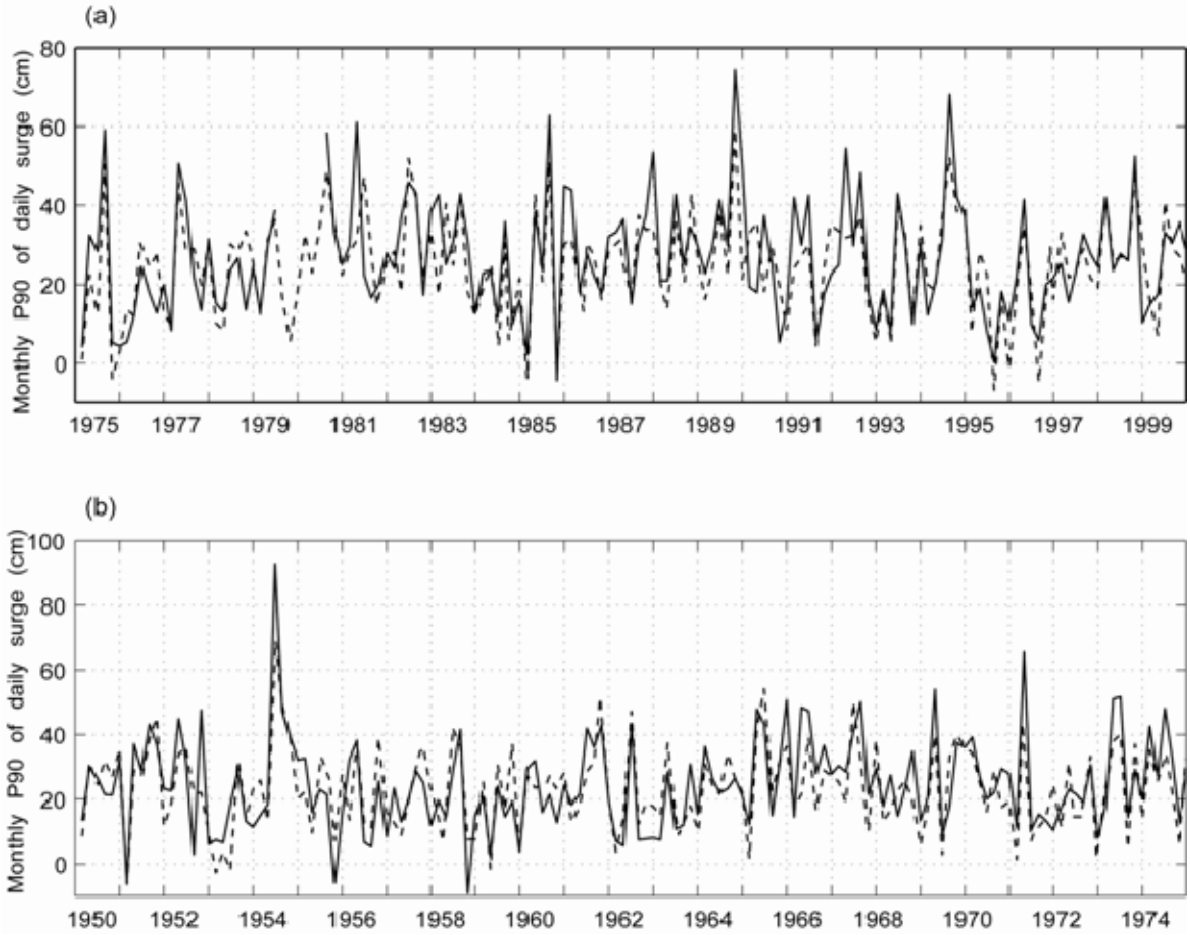

Figure 12. Time series of the monthly 90th percentile of daily surges at Oostende station as derived from *in situ* observation (full line) and estimated (dashed line) with the multiple linear regression and after inflation (a) When the regression is learned for the period 1950-1974 and tested for the period 1975-2000. (b) When the regression is learned for the period 1975-2000 and tested for the period 1950-1974.

	r (observation vs simulation)	RMSE (cm)	Mean (cm)		Std. (cm)	
			Obs	Sim.	Obs .	Sim.
P90 (1975-2000)	0.76***	7.9	32.1	30.2	14.2	14.8
P90 (1950-1974)	0.72***	7.6	28.2	26.8	13.5	13.9

Table 9. Goodness-of-fit statistics of the monthly 90th percentile estimated with the multiple linear regression and after inflation. In second line (third line), when the regression is learned for the period 1950-1974 (1975-2000) and tested for the period 1975-2000 (1950-1974). With the linear correlation (r), the roots mean square error (RMSE) and the standard deviation (Std). Three stars indicate the two-sided 99% level of significance according to a Student's t-test.

4.1.4 Wave height simulation

Highest surges and waves are associated with the same atmospheric pattern. A multiple linear regression (the same as in section 4.1.1) has also been tested to relate daily wave-height anomalies for the period 1994-2001 (for each year, daily wave-height anomalies are computed as the difference between the daily maximum wave height minus the yearly mean wave height) to *(1)* daily SLP averaged over the Baltic Sea and *(2)* daily value of the pressure gradient between the SLP averaged over the Baltic Sea and the Azores. Simulated daily wave-height anomaly time series has been inflated with the same methodology shown before (section 4.1.1).

	a	*b*	*cst*	*IF*
Wave (1994-2002)	-1.4	-1.6	1457.6	2.2

Table 10. Coefficient of the regression (*a, b* and *cst*) and coefficient of inflation (*IF*) for the regression using daily SLP averaged over the Baltic Sea and the daily value of the pressure gradient between the Baltic Sea and the Azores as predictors of daily surge-height anomaly at Westhinder.

At daily time scale, correlation between hindcasts and *in situ* observations is significant (r = r=0.58) over 99% level of confidence according to a Student t-test. Monthly 90th percentiles have then been extracted from the inflated daily wave-height anomaly time series computed by the regression and compared with *in situ* observations at Westhinder for the period 1994-2001). The agreement between observed and hindcast monthly 90th percentile is very strong (table 11, figure 13) showing the multiple linear regression also performs well the simulation of the inrterannual variability of highest waves along the Belgian coast.

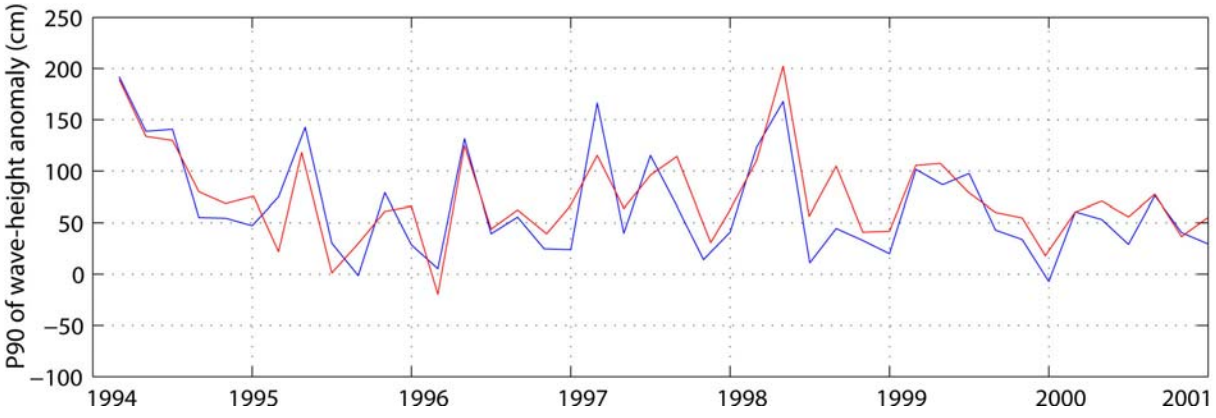

Figure 13. Time series of the monthly 90th percentile of wave-height anomaly at Westhinder for the period 1994-2001. *In situ* observation (blue line) and estimated (red line) with the linear regression using daily SLP averaged over the Baltic Sea and the daily value of the pressure gradient between the Baltic Sea and the Azores as predictors.

	Correlation (obs. vs hind.)	RMSE (cm)	Mean (cm)		Std. (cm)	
			Obs.	Sim.	Obs .	Sim.
Wave P90 (1994-2002)	0.72***	8.1	68.1	71.3	50	47.3

Table 11. Goodness-of-fit statistics of the monthly 90th percentile of wave-height anomaly estimated with the linear regression using daily SLP averaged over the Baltic Sea and daily value of the pressure gradient between the Baltic Sea and Azores as predictors and after inflation. With the linear correlation, the roots mean square error (RMSE) and the standard deviation (Std). Three stars indicate the two-sided 99% level of significance according to a random-phase test.

4.1.5 Statistical model for surge and wave-height simulation in the 21st century

In downscaling, small-scale phenomenon (i.e. weather variables or hydrodynamic phenomena) are related to large-scale quantities well resolved by GCM like SLP. The availability of different ensembles members with the same forcing of the scenario A1b (but with different model initialization) allows us to make more robust estimates of the model's forced response. The variability internal to an ensemble provides an estimate of the uncertainty associated with a single realization of forced climate response. Moreover, the availability of the two single SLP runs simulated with ARPEGE global circulation model allows us to consider one more optimistic (B2) and pessimistic (A2) climate change scenario than the medium scenario A1b and also to test an other GCM.

The linear regressions *(3)* designed in section 4.1 has been applied to the 17-ensembles runs of SLP and to A2 and B2 single runs. Each of the 17 daily surge-height time series has been inflated with the same methodology shown before. Values of *IF* are always between 1.59 and 1.6 which is almost similar to the *IF* computed for the period 1950-2000 between the daily surge-height time series observed at Oostende and simulated with the linear multiple regression using NCAR dataset. These results confirm that SLP variability is well simulated by ECHAM/MPI-OM and ARPEGE climate model (Van Ulden and Van Oldenborgh, 2006). These coefficients of inflations are then used to inflate daily surge-height time series until 2100, assuming that future climate variability in A1b, A2 and B2 scenarios would not change the ratio between the standard deviation of observations and simulations. The yearly 90th percentile is then computed from all resulting daily surge-height time series simulated for the period 1950-2100. First of all, on the historical period (1950-2000), simulations and observations at Oostende station show the same statistical skills (figure 13). The mean (respectively the standard deviation) of the yearly 90th percentile of surge, computed for each simulated surge-height time series, is always between 27.7 cm and 34.4 cm (respectively 5.5 cm and 8.7 cm), which is almost similar to the 30.2 cm (respectively 7.1 cm) computed with *in situ* observation at Oostende for the same period (figure 13).

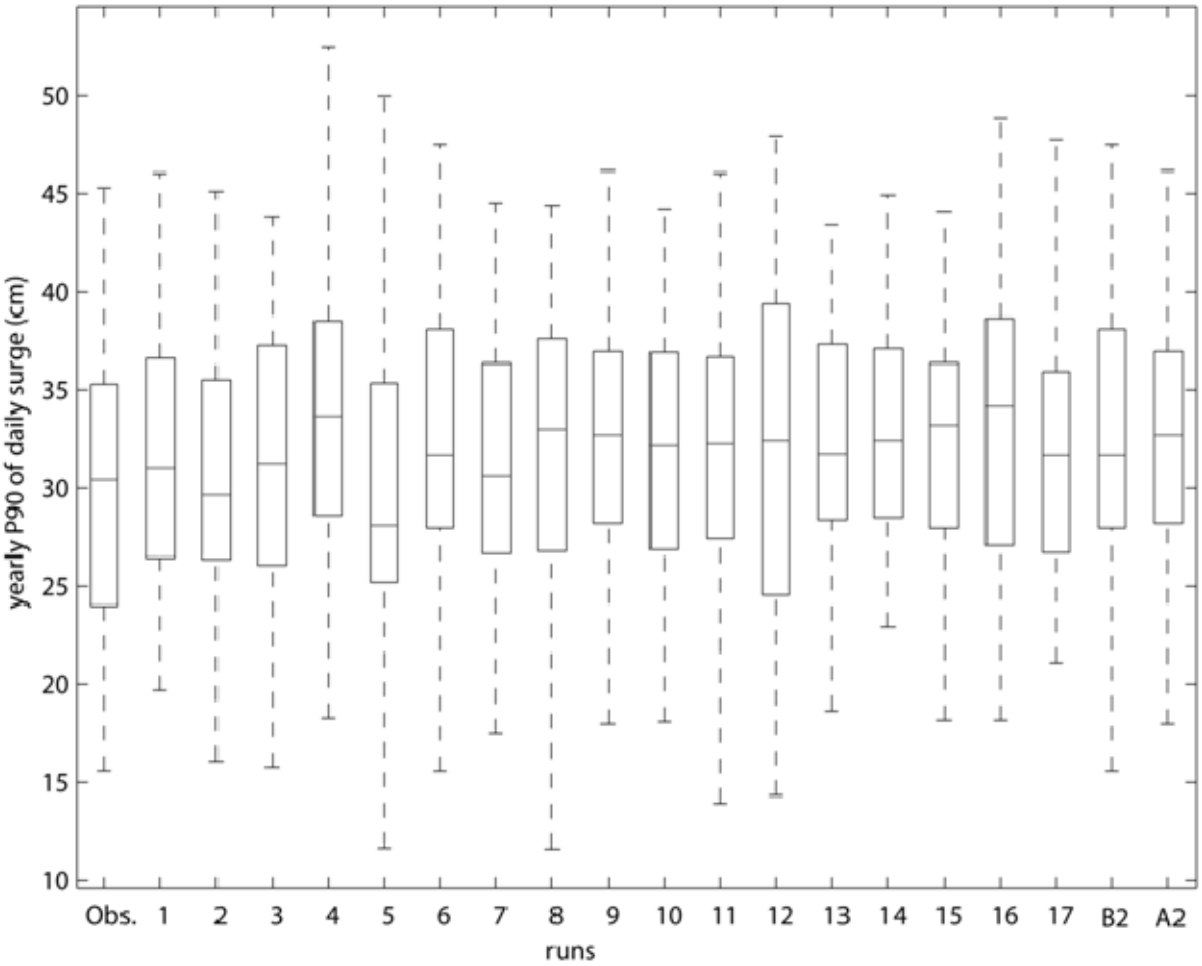

Figure 14. Box plot of the yearly P90 of surge height observed at Oostende (Obs.) and for the 17-ensembles time series simulated with the multiple linear regression for the period 1950-2000. With the five-number summaries: the smallest observation, lower quartile, median, upper quartile and the largest observation.

A Komolgorov-Smirnov test is used to compare the distribution of the observed yearly P90 time series at Oostende with each of the 19 simulated yearly P90 time series derived from the linear regression (17-ensembles runs A1b and A2 and B2 single runs). The test is also used to compare the simulated yearly P90 time series between each other. In fact, the Komolgorov-Smirnov test is one of the most useful and general methods for comparing two samples, as it is sensitive to differences in both location and shape of the empirical cumulative distribution functions of the two samples (Stephens, 1970). The null hypothesis of this test is that the two samples are drawn from the same distribution. In this case, the distributions considered under the null hypothesis are continuous distributions (Galen *et al*., 1986). The alternative hypothesis is that they have different continuous distributions. This test has the advantage of making no assumption about the distribution data and of giving a comparison between two samples based on the full distribution. Moreover, the Komolgorov-Smirnov test is here fully adapted to make a robust comparison between two time series which don't have the same chronology. According to this test, the distribution of each simulated yearly P90 time series is

never significantly different from the distribution of the observations. Moreover, distributions are also always similar within the simulated yearly P90 time series. It means that the linear regression used with SLP simulated by ECHAM/MPI-OM and ARPEGE climate models for the period 1950-2000 performs well the distribution of yearly P90 sea-surges at Oostende. Results are almost similar when validating wave-height simulation for the period 1994-2001 (not shown).

Then, over the 21st century, the yearly 90th percentile of surge could stay stationary along the Belgian coast under A1b, A2 and B2 climate change scenario, despite a weak multi-decadal variability (figure 14 and 15). For each 17-ensembles runs and for A2 and B2 single runs, the yearly 90th percentile of surge is averaged for three sub-period: 1950-2000, 2001-2050 and 2051-2100 (table 10). Values computed for the period 2050-2100 are never significantly different from those computed for the period 1950-2000 according to a Student's t test. Moreover, for each of the runs, the Komolgorov-Smirnov test is used to compare the distribution of the yearly P90 between each sub-period. No significant changes in the distribution were found between the two sub-periods. Moreover, results are similar when considering the wintertime P90 of wave-height anmolay (not shown).**To summarize, future climate change, from optimistic to pessimistic scenario, would not significantly modify storm-surge and wave-height characteristics along the Belgian coast**.

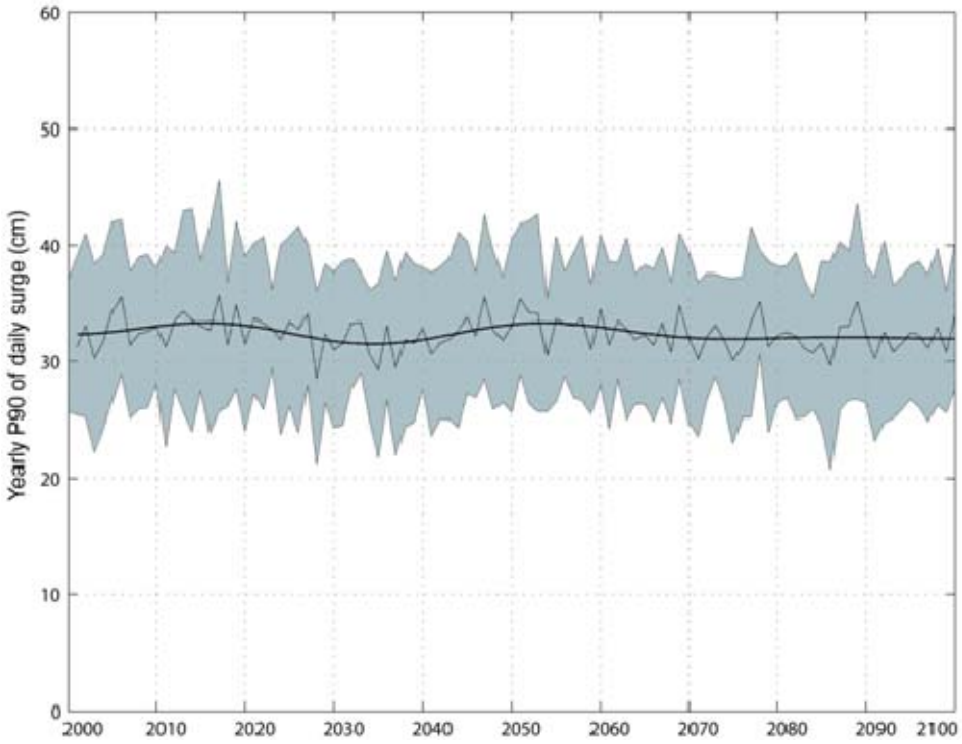

Figure 15. Thin line: average of the 17-ensembles time series of yearly 90th percentile of daily sea surge estimated with the linear multiple regression (2000-2100). Bold line: 30 year low-pass variations. The gray shading represents the variability within the 17-ensembles time series in each year (i.e. the yearly mean +/- σ).

	1950-2000	2001-2050	2051-2100
Oostende Obs.	30.2		
Run 1	31.5	31.3	31.2
Run 2	30.6	32.1	31.8
Run 3	31.7	31.9	31.2
Run 4	33.8	35.0	31.0
Run 5	28.7	34.8	31.8
Run 6	32.4	29.4	32.0
Run 7	31.3	31.8	32.5
Run 8	32.1	33.4	31.2
Run 9	31.9	31.3	32.1
Run 10	31.7	33.4	30.5
Run 11	31.4	32.5	32.3
Run 12	32.0	32.6	31.6
Run 13	32.3	31.8	31.4
Run 14	32.8	33.0	32.1
Run 15	32.3	30.8	31.4
Run 16	33.5	32.3	32.3
Run 17	31.6	32.8	32.6
A2	31.2	35.2	31.8
B2	32.1	34.1	33.3

Table 12. Yearly 90th percentile of daily sea surges averaged for three sub-periods and for the 17-ensembles time series computed with the multiple linear regression. Yearly P90 are averaged for three sub-periods: 1950-2000, 2001-2050, 2051-2100.

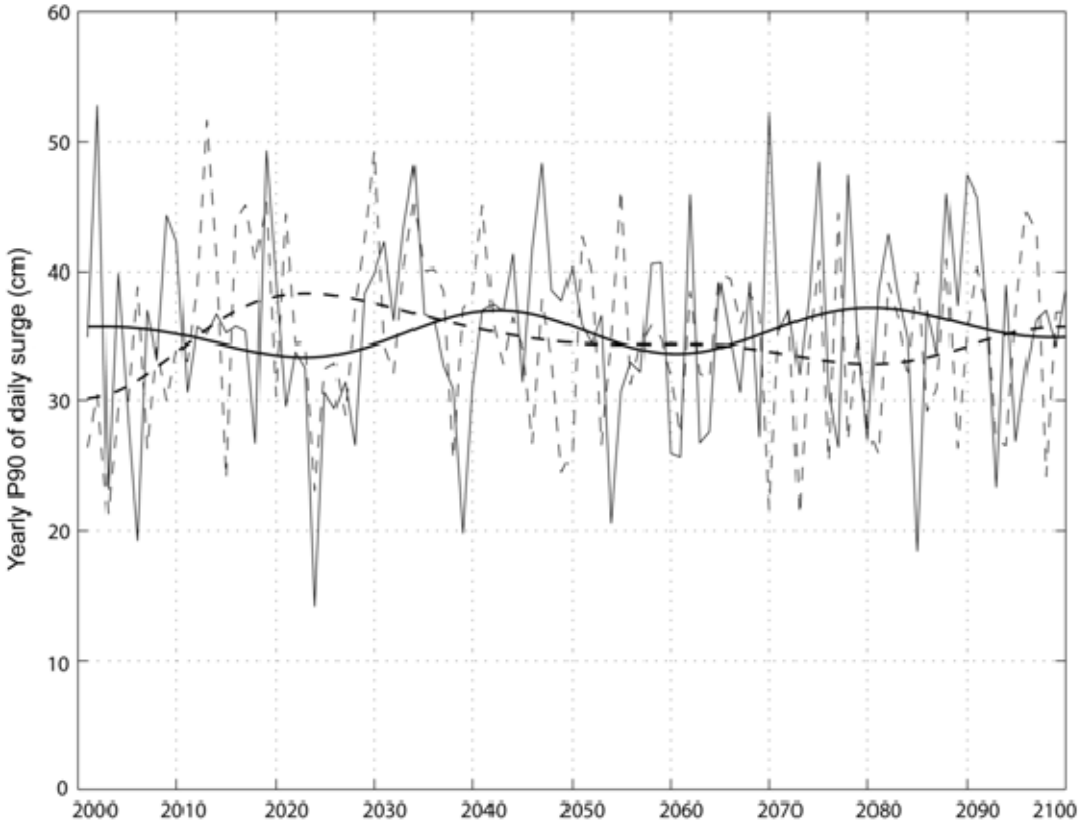

Figure 16. Yearly 90th percentile of daily sea surge estimated with the linear multiple regression (2000-2100) and for A2 (full line) and B2 (dashed line) SRES scenario, with the 30 year low-pass variations as superimposed bold lines.

4.2 WAQUA: present-day and future extreme sea-surges

A way to predict the future variability of extreme sea-surge height in the 21st century is to use regional-scale hydrodynamics models. In fact, even if linear statistical model, based on downscaling approach, performs well for simulating the interannual variability of highest surges, it usually underestimates the most extreme values. It's a recurring and normal skew of the linear statistical models. For studies needy in extreme values analysis such as the calculation of return periods for extreme levels, it's thus more advised to use hydrodynamics models. The basic ensemble of 17 runs of 10-minutes surge-height time series simulated at Oostende with WAQUA from 1950 to 2100 is used here to analyze potential changes in extreme sea-surge under A1b climate change scenario.

Return period of surge height have been computed at Oostende station for *in situ* observations and for the 17-ensembles WAQUA's surge-height time series. We follow the common choice in empirical studies to fit the annual maxima to Generalized Extreme Value (GEV) distribution (Cole, 2001), and plot the results on a Gumbel plot. Note that this method is usually used for hydro-meteorological data such as sea surges (Pirazzoli and Tomasin, 2007, van den Brink *et al*., 2004). The R (R Development Core Team, 2006) package "extremes"

(Gilleland and Katz, 2005) has been employed. For the period 1950-2000, return periods are computed with in situ observation at Oostende and compared with return periods computed with the total WAQUA set for the same period (i.e. the total set of the annual maxima of surges of the 17 WAQUA's surge-height time series for the period 1950-2000). Figure 16 shows the return level plots of GEV distribution with the 95% confidence intervals. Results shown a good agreement between the GEV distributions fitted to the observed and WAQUA's surges (figure 16). The GEV location parameter μ (representing the surge level with an exceedance probability of once a year) estimated from WAQUA (=86.2 cm) equals that of the observational record (=85.5 cm) within 1 cm. This implies that systematic differences between the observed data and WAQUA's simulation are small. Moreover, for the period 1950-2000, 10 to 10^2-years return periods of annual maxima of surges computed with *in situ* observations are almost similar to those computed with the total WAQUA's set (table 11). To summarize, WAQUA hydrodynamic model performs well in simulating extreme surges along the Belgian coast.

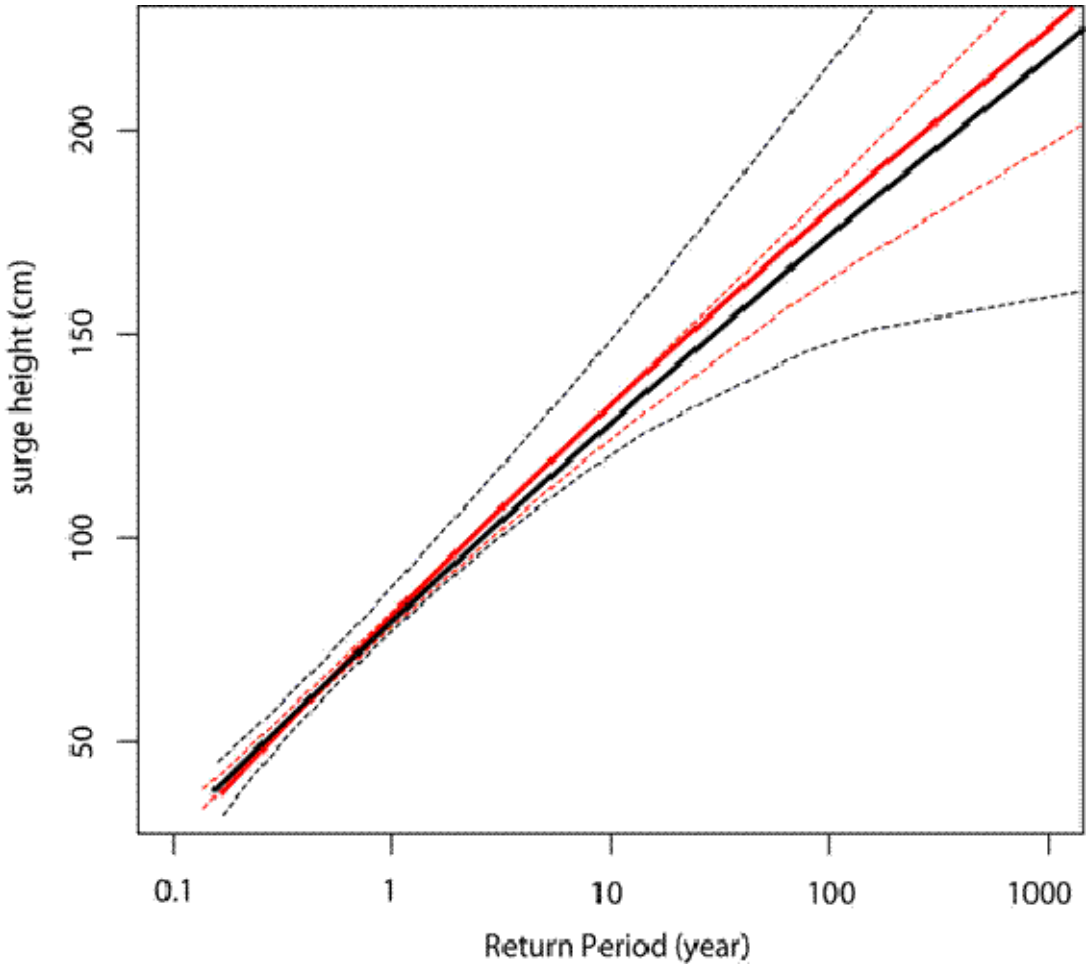

Figure 17. Return level plots and estimated 95% confidence intervals for annual maxima obtained with the GEV distribution at Oostende station for the period 1950-2000. *In situ* observation in black lines and for the total WAQUA set (i.e. the total set of the 17-esembles time series) in red lines.

	10 years	50 years	100 years
Oostende observations 1950-2000	125 cm	150 cm	175 cm
Total WAQUA 1950-2000	127 cm	154 cm	180 cm

Table 13. Return period levels of annual maxima sea surges at Oostende station computed for the period 1950-2000 and obtained with GEV distribution for *in situ* observation(second line) and for the total WAQUA set, corresponding to the total of the 17-esembles time series (third line).

Return period of annual maxima of surges at Oostende are then computed for the period 2050-2100 with the total WAQUA set. Figure 17 shows the return level plots of GEV distribution with the 95% confidence intervals for *in situ* observation for the period 1950-2000 (black lines), for WAQUA's surges on the same period (red lines) and for WAQUA's surges for the period 2050-2100 (blue lines). The GEV location parameter μ estimated from WAQUA for the period 2050-2100 (=85.8 cm) equals that computed for the period 1950-2000 (=86.2 cm) within 1 cm, meaning that systematic differences between the two sub-periods are small. Moreover, return period levels (from 10 to 10^2 –years) computed for the period 2050-2100 nearly equal those computed for the period 1950-2000 (table 12). Climate change in A1b scenario would obviously not significantly modified return periods of extreme surges along the Belgian coast.

Note that the same analyses have been done using the ensemble of 17 runs of total sea-level height, including astronomical tide forcing. In fact, some recent studies show that the nonlinear interaction between tide and surge could be important (Horsburgh and Wilson, 2007). This interaction could play a role in the distribution of the surge height in the North-Sea and act to reduce maximum water levels (Horsburgh and Wilson, 2007). Results are almost similar than results found with only the surge component and show not **significant changes in extreme sea level during the 21st century in A1b climate change scenario** (not shown).

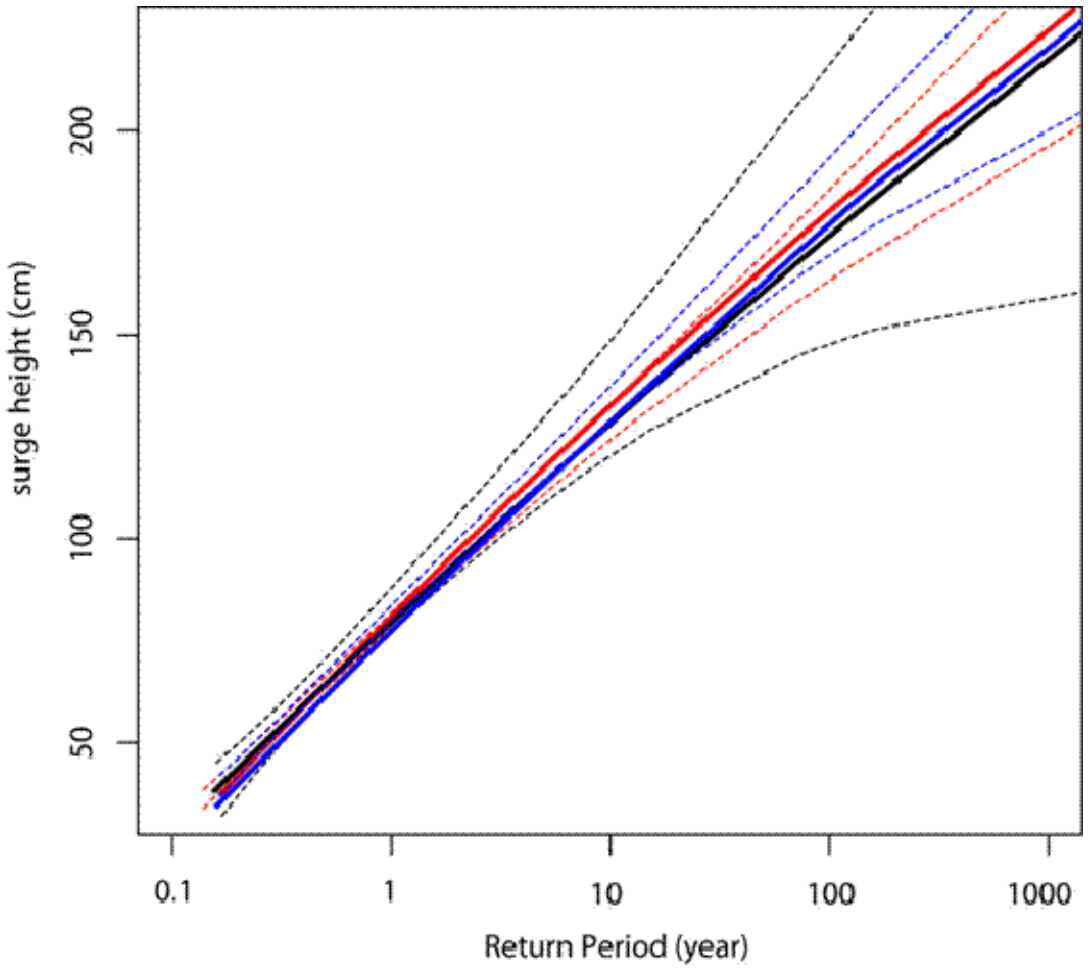

Figure 18. Return level plots and estimated 95% confidence intervals for annual maxima obtained with the GEV distribution at Oostende. For *in situ* observations for the period 1950-2000 (black lines). For WAQUA total set for the period 1950-2000 (red lines) and for WAQUA total set for the period 2050-2100 (blue lines).

	10 years	50 years	100 years
Total WAQUA 1950-2000	127 cm	154 cm	180 cm
Total WAQUA 2050-2100	125 cm	152 cm	178 cm

Table 14. Return period levels of annual maxima sea surges at Oostende station obtained with GEV distribution for the total WAQUA set for the period 1950-2000 (second line) and for the period 2050-2100 (third line).

4.3 Surge-related atmospheric conditions: variability in the 21st century

During the 21st century, the yearly mean SLP over the Baltic Sea stays almost stationary (figure 18a). Even if the daily to interannual variability of surge at Oostende is quasi exclusively associated with SLP variability over the Baltic Sea, the SLP variability over the Azores could play a role over the long-term by modifying the strength of the pressure gradient between the Azores and the Baltic Sea. In other words, the SLP variability over the Azores could change the strength and direction of the atmospheric circulation over western Europe and affect surges at local scale (Ullmann and Monbaliu, 2009). That's why it's important to have a large-scale view to analyze long-term changes in sea surges at local and regional scale (Ullmann and Moron, 2008). The behavior of SLP near the Azores stays almost stationary in each 17-ensembles runs under A1b SRES scenario (figure 18b). The yearly frequency of days associated with a strong pressure gradient between low pressure > 990 hPa over the Baltic Sea and high pressure > 1020 hPa over the Azores stays logically stationary during the same period (figure 18c). No significant long-term trend has been found within the 17-ensembles runs. The same results are observed when considering the two single runs A2 and B2 (not shown). It means that in each storyline for the future climate considered in this study, from B2 to A2 and through A1b, climate change (i.e. external forcing as GHG) would not significantly modified the strength and the frequency of the surge-related North-Westerly atmospheric flow in the southern part of the North Sea. Moreover, as highest sea surges and waves are associated with the same atmospheric patterns (i.e. the same barometric gradient), it means also that **climate change in B2, A1b and A2 scenarios could not significantly modify wave heights along the Belgian coast in the next century.**

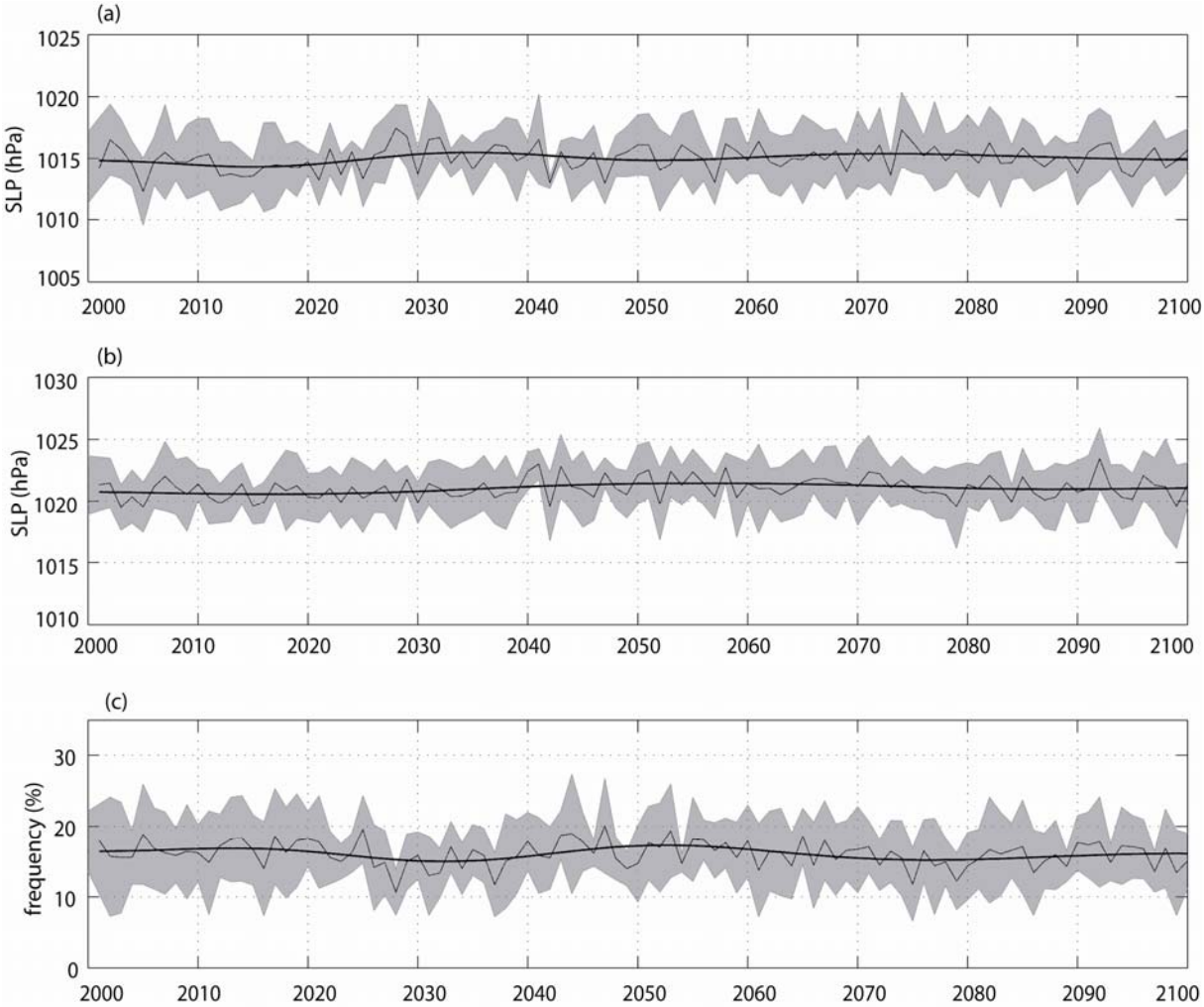

Figure 19. Thin line: average of the 17-ensembles time series of yearly mean SLP (a) over the Baltic Sea ([15°E-20°E], [50°N-55°N]), (b) over the Azores ([30°W-0°W], [35°N-45°N]) and (c) of the frequency of daily SLP over the Baltic Sea < 990 associated with SLP > 1020 over the Azores (2000-2100). Bold line: 30 year low-pass variations. The gray shading represents the variability within the 17-ensembles time series in each year (i.e. the yearly mean +/- σ).

5 Conclusion

Global circulation climate models (GCMs) are used to produce numerical simulation of several climate variables in different scenarios of greenhouse gases emission. However, they are designed to simulate climate conditions at several hundred kilometers scale. These models are thus not always reliable below this scale and regional coastal systems are not resolved sufficiently. A way to resolve this problem is downscaling techniques, based on statistical relationships between global and regional parameters.

A statistical downscaling was used to relate sea-level pressure to surge and wave height along the Belgian coast. Results show that climate change under B2, A1b and A2 scenarios would obviously not significantly modified the frequency and height of sea-surge and highest waves

along the Belgian coast. In fact, in these SRES scenarios, the frequency of strong northwesterly atmospheric flow over the southern part of the North Sea could stay stationary during the 21st century. Significant wave height could thus also stay stationary during the next century. These results complete those found by Sterl *et al*. (2008) and Van den Hurk *et al*. (2006) showing no significant changes in wind speed and sea-surge height along the Dutch coast in future climate. Moreover, these results confirm that climate change would not significantly modified extreme surges and winds in the southern part of the North Sea region (Debenard and Roed, 2007). To summarize, following these results and previous studies, there is no reason to foresee changes in atmospheric circulation in the southern part of the North-Sea and in extreme storm-surge and wave height until the end of the 21st century. Note that the multiple linear regression designed in this work can be easily used with other GCMs and other climate change scenario helping the surge-height prediction which is required for impact calculation.

Despite the possible stationary of surge and wave height in a future climate, the mean sea-level rise will ineluctably increase the frequency and height of extreme sea levels and waves during storm events, which is particularly important in an impact perspective, especially for coastal defense. In other words, even if storms events in the southern part of the North Sea won't change, they will occur on a mean sea level progressively higher and higher. In fact, IPCC predict a global mean sea-level rise between + 1 mm/yr and + 9 mm/yr for the 21st century. A regional scale, in the southern North Sea, the Belgian National Commission for Climate Change (2006) estimates a mean sea-level rise between a minimum of + 1.4 mm/yr and a maximum of + 9.3 mm/yr depending on the climate change scenarios. A speed of + 20 mm/yr is also considered as the worst case scenario but nevertheless very not probable. Moreover, the Delta commission of the Netherlands predicts a mean sea-level rise between + 5.5 mm/yr and + 11 mm/yr for the North-Sea based on the KNMI Climate Change Scenarios 2006 for the Netherlands (Van den Hurk *et al*., 2006).

Following this study and according to the CLIMAR climate change scenarios for the 21st century (section 1.1), we decide to keep here two scenarios for the Belgian coast (table 13). The first one is a medium scenario (M) with no changes in storminess and storm-related surges and waves and with in medium rate of sea-level rise of +6.0 mm/year (i.e. +60 cm until 2100) (table 13). The second one is a warm scenario (W) with still no changes in storminess but with an accelerated mean sea-level rise with a mean rate of +9.3 mm/year (i.e. +93 cm until 2100) which correspond to the upper rate of the IPCC's estimations.

	M	W
Change in storminess (Wind velocity, surges, wave height)	No	No
Mean sea-level rise	+60 cm	+93 cm

Table 15. Scenarios of climate change for the 21st century and sea-level rise estimate until 2100 and storminess related variability.

However, study and prediction of climate change impacts on regional coastal systems has to deal with large uncertainties. Uncertainties come first from storminess because clear relations between local key processes and large scale climate variability are difficult to obtain. Further problems occur because a changing climate may cause changes in the relationship between global and local parameters use to predict storminess at regional scale. The assessment of local impacts is therefore very difficult. Then, although the future mean sea-level rise will be mainly linked with the increase of the sea surface temperature, several other parameters could play a role, especially at regional scale: oceanic circulation, salinity and the huge quantity of continental ice melting which are still difficult to predict. A worst scenario with a mean sea-level rise of +200 cm until 2100 (+20 mm/years) has been proposed by Brooks *et al.* (2006). We considered reasonably this scenario as strongly unexpected, but still possible in case of massive ice melting of ice sheets and the stopping of the thermohaline Ocean Circulation

Acknowledgements

This study is partly funded by the European Commission 2005-2009 under SEAMOCS (Applied stochastic models for ocean engineering, climate and safe transportation) Research Training Network. This study is also part of the QUEST4D project (Quantification of erosion and sedimentation patterns to trace the natural versus anthropogenic sediment dynamics) funded by the Belgian Science Policy (SD/NS/06B). The ESSENCE project, lead by Wilco Hazeleger (KNMI) and Henk Dijkstra (UU/IMAU), was carried out with support of DEISA, HLRS, SARA and NCF (through NCF projects NRG-2006.06, CAVE-06-023 and SG-06-267). We thank the DEISA Consortium (co-funded by the EU, FP6 projects 508830 / 031513) for support within the DEISA Extreme Computing Initiative (www.deisa.org). T

6 Reference

Alexandersson H., Tuomenvirta H., Schmith T., Iden K., 2000. Trends of storms in NW Europe derived from an updated pressure data set. *Clim. Res*., 14: 71-73.

Brooks, N., R. Nicholls & J. Hall, 2006. Sea level rise: coastal impacts and responses. Externe Expertise für das WBGU-Sondergutachten "Die Zukunft der Meere – zu warm, zu hoch, zu sauer", Berlin, 46 pp.

Butterworth S., 1930. On the theory of filter amplifiers. *Wireless Engineer*, 7:536-541.

Cabanes C., Cazenave A., Le Provost C., 2001. Sea level rise during past 40 years determined from satellite and in situ observations. *Science*, 294: 840-842.

Cazenave A., Nerem R.S., 2004. Present-day sea level change: observations and causes. *Rev. Geophys.*, 42, RG3001, doi: 10.1029/2003RG00139.

CLIMAR: Impact of climate change on the physical and chemical parameters of the North Sea. *Literature study*, p. 70, 2007.
Coles S., 2001. An introduction to statistical modeling of extreme values. Springer, London.

Debernard J., Roed L.P., 2007. Future wind, wave and storm surge climate in the Northern Seas: a revisit. Tellus, 60: 427-438.

Galen R. Shorack et Jon A. Wellner, Empirical Processes With Applications to Statistics, John Wiley & Sons Inc, 1986, 976 p. (ISBN 047186725X).

Gilleland E., Katz R.W., 2005. Extremes toolkit (extremes): weather and climate applications of extreme value statistics. http://www.assessment.ucar.edu/toolkit.

Heyen H., Zorita E., von Storch H., 1996. Statistical downscaling of monthly mean North-Atlantic air pressure to sea level anomalies in the Baltic sea. *Tellus*, 48A: 312-323.

Horsburgh K.J., Wilson C., 2007. Tide-surge interaction and its role in the distribution of surge residuals in the North-Sea. *J. Geophys. Res.*, 112, C8003, doi: 10.1029/2006JC004033.

Hurrell J.W., Van Loon H., 1997. Decadal variations in Climate associated with the north Atlantic deviation. *Climatic change*, 36: 301-326.

Huth, R., 1999: Statistical downscaling in central Europe: Evaluation of methods and potential predictors. *Climate Res.*,13: 91-101.

IPCC, 2007. Climate Change 2007. The Physical Science Basis. *Cambridge University Press*, Cambridge, 940 p.

Jungclaus, J.H., Botzet M., Haak H., Keenlyside N., Luo J.J., Latif M., Marotzke J., Mikolajewicz U., Roeckner E., 2006. Ocean circulation and tropical variability in the coupled model ECHAM5/MPI-OM. *J. Clim.*, 19: 3952-3972.

Kalnay et al.,The NCEP/NCAR 40-year reanalysis project, *Bull. Amer. Meteor. Soc.*, 77: 437-470, 1996.

Lambeck C., 1990: Late Pleistocene, Holocene and present sea-levels: constraints on future change. *Global and Planetary Change*, 3: 205-217.

Langenberg H., Pfizenmayer A., Von Storch H., Sundermann J., 1999. Storm-related sea level variations along rthe North Sea coast: natural variability and anthropogenic change. *Cont. Shelf Res.*, 19: 821-842.

Lowe J.A., Gregory J.M, Flather R.A., 2001. Changes in the occurrence of storm surge in the United Kingdom under a future climate scenario using a dynamic storm surge model driven by the Hadley Center climate models. *Clim. Dyn*., 18: 197-188.

Machel H., Kappla A., Flohn H., 1998. Behaviour of the centres of action above the Atlantic since 1881, Part 1, characteristics of seasonal and interannual variability. *Int J. Climatol,* 18: 1-22.

Marlsand S.J., Haak H., Jungclaus J.H., Latif M., Roske F., 2003. The Max-Planck-Institute global ocean/sea ice model with orthogonal curvilinear coordinates. *Ocean Modelling*, 5: 91-127.

Michaelsen J.M., 1987. Cross-validation in statistical climate forecast models. *Jour. Of applied Meteo*., 26: 1589-1600.

Nerem R.S., Mitchum G.T., 2001. Observations of sea level change from satellite atltimetry. Sea level rise: history and consequence, *Academic press*, San Diego, 121-163.

Orlanski I., 1975. A rational subdivision of scales for atmospheric processes. *Bulletin of the American Meteorological Society*, 56: 527-530.

Petersen M., Rohde H., 1991. Sturmluft. Die großen Fluten an den Küsten Schleswig Holsteins und der Elbe. Neumünster.

Pirazzoli P.A., 2000. Surges, atmospheric pressure and wind change and flooding probability on the Atlantic coast of France. *Oceanologica Acta,* 23: 643-661.

Pirazzoli P.A., Costa S., Dornbusch U., Tomasin A., 2005. Recent evolution of surge-related event and assessment of coastal flooding risk on the eastern coasts of the English Channel. *Ocean dyn*., 56: 498-512.

Pirazzoli P.A., Tomasin A., 2007. Estimation of return periods for extreme sea levels: a simplified empirical correction of the joint probabilities method with examples from the French Atlantic coast and three ports in the southwest of the UK. *Ocean Dyn.*, 57: 91-107.

Pugh D.T. (1987). Tides, surges and mean sea level. *John Wiley & Sons Eds*. 488 p.

R Development Core Team, 2006. R: a language en environment for statistical computing. R Foundation for Statistical Computing, Vienna, Austria. ISBN 3-900951-07-0. http://www.R-project.org

Rodwell M.,J., Rowell D.P., Folland C.K., 1999. Oceanic forcing of the wintertime North Atlantic Oscillation and European climate. *Nature*, 398:320-323.

Royer J.F., Cariolle D., Chauvin F., Déqué M., Douville H., Hu R.M, Planton S., Rascol A., Ricard J.L., Melia D.S.Y., Sevault F., Simon P., Somot S., Tyteca S., Terray L., Valcke S. (2002). Simulation des changements climatiques au cours du XXIème siècle incluant l'ozone stratosphérique. *Compte Rendus Geoscience*, 334: 147-154.

Siegismund F., Schrum C., 2001. Decadal vareiability of the wind field in the North Sea. *Climate research*, 18: 39-45.

Stephens, M. A. "Use of the Kolmogorov-Smirnov, Cramer-Von Mises and Related Statistics Without Extensive Tables." *Journal of the Royal Statistical Society*. Series B, Vol. 32, No. 1, 1970, pp. 115–122.

Sterl A., Van den Brink H., Haarsme R., Meijgaard E., Vries H., 2008. North Sea winds and storm surges. *Workshop DeltaCie*, Amsterdam, 07 April 2008.

Sterl A., Severijns C., van Oldenborgh G.J., Dijkstra H., Hazeleger W., van den Broeke M., Burgers G., van den Hurk B., van Leeuwen P.J., van Velthoven P., 2008. When can we expect extremely high surface temperatures? *Geophys. Res. Lett.*, 35, (2008), L14703 doi: 10.1029/2008GL034071

Svensson C., Jones D.A., 2002. Dependence between extreme sea surge, river flow and precipitation in eastern Britain. *Int. J. Climatol.*, 22: 1149-1168.

Technum-IMDC-Alkyon, 2002. Hydrodynamic boundary conditions for the water levels and storm surge conditions to support the redesign of the coastal protection and to increase the harbor access at Oostend (in Dutch). *Study report for the Flemish Government of Belgium*, Administration AWZ Afdeling Waterwegen Kust.

Tsimplis M.N., Rixen M., 2002. Sea level in the Mediterranean Sea: the contribution of temperature and salinity changes. *Geophys. Res. Letters*, 29, doi:10.1029/2002GL015870

Trigo I.F., Davies T.D., 2002. Meteorological conditions associated with sea surges in Venice: a 40 year climatology. *International Journal of Climatology*, 22: 787-803.

Ullmann A., Monbaliu J., 2009. Changes in atmospheric circulation over the North Atlantic and sea surge variations along the Belgian coast during the 20th century. *International Journal of Climatology*. In press.

Ullmann A. Moron V., 2008. Weather regimes and sea surge variations over the Gulf of Lions during the 20th century. *Int. J. of Climatol.*, 28: 159-171.

Van den Brink H.W., Konnen G.P., Opsteegh J.D., van Oldenborgh G.J., Burgers G., 2004. Improving 10^4-year surge level estimates using data of the ECMWF seasonal prediction system. *Geophysical Research Letters*, 31, L17210, doi:10.1029/2004GL020610.

Van den Eynde, D., F. Francken, S. Ponsar en J. Ozer, 2008. Bepaling van de primaire impacten van klimaatsverandering: statistische analyse van metingen van golven, windsnelheid en –richting en van zeewatertemperatuur. Technisch Rapport CLIMAR/X/DVDE/200807/ NL/TR4, *Rapport voorbereid in het kader van het CLIMAR project*, uitgevoerd voor Federaal Wetenschapsbeleid, Contract SD/NS/01A, Beheerseenheid van het Mathematisch Model van de Noordzee, 40 pp. (Annex 1-04).

Van den Hurk B., Klein Tank A., Lenderink G., van Ulden A., van Oldenborg G.J., Katsman C., van den Brink H., Keller F., Bessembinder J., Burgers G., Komen G., Hazelegers W., Drifhout S., (2006). KMNI Climate Change scenarios 2006 for the Netherlands. *KNMI scientific report,* WR 2006-01, Utrecht.

Van Oldenborgh G.J., Philip S.Y., Collins M., 2005. El Nino in a changing climate: a multi-model study. *Ocean Science*, 1: 81-85.

Von Storch H., Zwiers F.W., 1999. Statistical analysis in climate research. *Cambridge Univ. Press*. 494 p.

Von Storch H., Reichardt H., 1997. A scenario of storm surge statistics for the German bight at the expected time of doubled atmospheric Carbon Dioxide concentration. *J. Climate*, 10: 2653-2662.

Van Ulden A., Van Oldenborgh G.V., 2006. Large-scale atmospheric circulation biases and changes in global climate model simulations and their importance for regional climate scenarios: a case study for West-Central Europe. *Atmos. Chem. Phys.*, 6: 863-881.

Wakelin S.L., Woodworth P.L., Flather R.A., Williams J.A., 2003. Sea-level dependence on the NAO over the NW European continental shelf, *Geophys. Res. Letters*, 30, doi:10.1029/2003GLO17041.

Weisse R., Von Storch H., Feser F., 2005. Northeast Atlantic and North Sea storminess as simulated by regional climate model 1958-2001 and comparison with observations. *J. Climate*, 18: 465-479.

http://www.ecmwf.int

http://dss.ucar.edu/